

Research Article

The geography and progression of blowouts in the coastal dunes along the eastern shore of Lake Michigan since 1938

Kevin G. McKeegan^a  and Alan F. Arbogast^b

^aU.S. Geological Survey, Center of Excellence for Geospatial Information Science, 1400 Independence Rd, Rolla, MO 65401, United States and ^bDepartment of Geography, Environment, and Spatial Sciences, Michigan State University, Geography Building, 673 Auditorium Rd, East Lansing, MI 48824, United States

Abstract

Coastal dunes along Lake Michigan's eastern shoreline are a unique system comprising perhaps the largest complex of freshwater coastal dunes in the world. Here, we examine the blowouts in this region and determine how they have evolved since the 1930s. We conducted a spatiotemporal analysis of 435 blowouts by comparing repeat aerial images of the coast beginning in 1938. Using an unsupervised machine learning classification known as iso-clustering, we mapped blowout morphologies at three timestamps: 1938, 1986–1988, and 2018. We then compared the blowout geographies through a technique known as a spatial-temporal analysis of moving polygons (STAMP) model, which allowed us to analyze how each blowout changed in time and space. Results show blowouts have contracted ~37% in size since 1938, mostly at the expense of vegetation, with many fragmenting. These findings comport with other regional and global studies detailing a trend in coastal dune stabilization from vegetation and suggest that an increase in precipitation or other environment drivers could be responsible. Moreover, we detected no new blowouts since 1938 along the ~500 km shoreline or on any of the Lake Michigan islands. This suggests blowouts here are artifacts of premodern conditions, perhaps the result of prior stormier or drier eras.

Keywords: Coastal dunes, Blowouts, Dunes, Lake Michigan, Geomorphology, Aeolian geomorphology, Ecogeomorphology, Aerial photography

(Received 14 July 2022; accepted 13 February 2023)

INTRODUCTION

Coastal sand dunes adjoin much of the eastern shore of Lake Michigan and collectively comprise possibly the largest freshwater coastal dune system in the world (Peterson and Dersch, 1981) (Figure 1). A unique coastal system, these dunes line the shore for several kilometers along numerous parts of the coast and often extend up to a kilometer inland (Sanford, 1916; Buckler, 1979). Some dunes exceed 50 m in height and contain enormous volumes of sand (Arbogast et al., 2009). Unlike dune systems on marine coasts, Lake Michigan's coastal dunes developed without the influence of tectonic or tidal activity (Hansen et al., 2010). On the contrary, they are the product of many factors, but primarily are the result of the reworking of sandy glacial and lacustrine deposits in response to climatic and lake level variability (Loope and Arbogast, 2000; Hansen et al., 2010; Thompson et al., 2011; Lovis et al., 2012). The subsequent dune environments found in the eastern Lake Michigan basin are thus a subject of this variability, resulting in progradational or aggradational aeolian landforms depending upon the geomorphological setting along the ~550 km shoreline (Buckler, 1979; Wilson, 2001; Lepczyk and Arbogast, 2005; Lovis et al., 2012; Kilibarda et al.,

2014; Paskus and Enander, 2019). Within these settings along the coastline, dune blowouts are common aeolian features (Buckler, 1979). These erosional landforms, in which portions of a dune are “blown out” due to wind erosion, are known markers of climatic and anthropogenic dunefield conditions (Hesp, 2002). Thus, dune blowouts, the subject of this paper, represent an important area of scientific study.

Dune building at many sites in the Lake Michigan region, especially those toward the southern end of the lake basin, apparently began ca. 5.5 ka amidst an ~1,500-year period of elevated lake levels on ancestral Lake Michigan-Huron, known collectively as the Nipissing transgressions (ca. 6–4.5 ka) (Larsen, 1987; Thompson et al., 2011; Lovis et al., 2012). At the apex of the Nipissing transgressions was the Nipissing high stand, a period of maximum water height (~178–183 m) (Dott and Mickelson, 1995; Baedke and Thompson, 2000; Thompson et al., 2011). The high stand may have occurred as early as ca. 5.5 ka (Lewis, 1969; Petty et al., 1996; Lovis et al., 2012) or as late as ca. 4.5 ka (Larsen, 1987; Hansel and Mickelson, 1988; Thompson and Baedke, 1997; Baedke and Thompson, 2000; Thompson et al., 2011; Fisher et al., 2012). Regardless, the Nipissing high stand immediately preceded a relatively sudden drop in lake levels, ~4 m during ca. 1,200 years (Baedke and Thompson, 2000), driven primarily by the effects of isostatic rebound on downstream lake outlets (Monaghan et al., 1986; Larsen, 1987; Bishop, 1990; Baedke and Thompson, 2000; Lovis et al., 2012), although changes

Cite this article: McKeegan KG, Arbogast AF (2023). The geography and progression of blowouts in the coastal dunes along the eastern shore of Lake Michigan since 1938. *Quaternary Research* 115, 25–45. <https://doi.org/10.1017/qua.2023.10>

© University of Washington. Published by Cambridge University Press, 2023. This is an Open Access article, distributed under the terms of the Creative Commons Attribution-NonCommercial-ShareAlike licence (<https://creativecommons.org/licenses/by-nc-sa/4.0/>), which permits non-commercial re-use, distribution, and reproduction in any medium, provided the same Creative Commons licence is included and the original work is properly cited. The written permission of Cambridge University Press must be obtained for commercial re-use.





Figure 1. Overview map of eastern Lake Michigan dunefields.

in regional climate also may have played a role (Hansel and Mickelson, 1988; Petty et al., 1996). After this sudden decline, lake levels fluctuated around the 1819–1999 modern mean of 176.7 m, often in apparent cycles (Baedke and Thompson, 2000).

Periods of aeolian activity on the eastern lakeshore continued thereafter from the Nipissing High Stand, followed by brief intervals of dune stabilization (Van Oort et al., 2001; Arbogast et al., 2002; Hansen et al., 2002, 2010; Lepczyk and Arbogast, 2005; Blumer et al., 2012; Lovis et al., 2012; Kilibarda et al., 2014). Yet, this overall pattern was not uniform and some nonlinear spatiotemporal and geomorphological variability in dunefields exists between the northern and southern portions of the lakeshore (Lovis et al., 2012; Fulop et al., 2019). Nevertheless, several studies have identified periods of aeolian activity and stability since the embryonic stages of dune formation, which mostly occurred during the Nipissing transgressions. In their study of coastal dunes along the southern half of Lake Michigan's eastern shoreline, Hansen et al. (2010) identified six aeolian phases beginning from the most recent deglaciation, which began ca. 14 ka in the southern Lake Michigan basin and ended ca. 11 ka when ice cleared the Straits of Mackinac (Kincare, 2007), through to present day. Similarly, Kilibarda et al. (2014) noted four phases of

dune and coastal evolution on the southern reaches of Lake Michigan beginning at ca. 6 ka. Lovis et al. (2012) detected a series of aeolian periods that varied in a spatiotemporal manner delineated primarily by the isostatic hinge line, north of which dunefields developed somewhat differently due to ongoing crustal rebound and other factors.

Although different, all three studies (Hansen et al., 2010; Lovis et al., 2012; Kilibarda et al., 2014) identified a pronounced Late Holocene episode of regional dune stability called the Holland Interlude, a period marked by vegetation expansion across the previously mobile coastal dunes. This period of stability resulted in pedogenic formation of the Holland Paleosol, an Inceptisol present in dunes along Lake Michigan's southeastern coast (Arbogast et al., 2004; Hansen et al., 2006). The studies disagreed on the approximate dates of the so-called Holland Interlude, ranging from ca. 3 ka to ca. 0.5 ka, but agreed that the dates overlapped for a period from ca. 1.6–1 ka (Hansen et al., 2010; Lovis et al., 2012; Kilibarda et al., 2014). Whatever the exact chronology, these distinct, identified aeolian phases were likely driven by a complex system of climate and lake-level changes, which either increased or restricted the supply of sand.

Recently, White et al. (2019) and McKeehan and Arbogast (2021) identified a modern trend toward dune stabilization

along Lake Michigan's eastern shoreline by documenting the expansion of vegetation through an object-based analysis of aerial imagery and ground-level repeat photography, respectively. If true, these two findings could signal a new phase for the region's coastal dunefields (White et al., 2019; McKeehan and Arbogast, 2021). This phenomenon was also implied by Lovis et al. (2012, p. 117), who noted a decreased sand supply in the regional coastal aeolian system over the last 500 years. Regional dune stabilization could also suggest that a new mesoscale climate regime has begun to evolve across the Great Lakes (Yurk and Hansen, 2021). Close observation of the trends and environments of Lake Michigan coastal dune systems could help us determine if this shift is underway.

As Ritchie (1972, fig. 12) demonstrated, the aeolian conditions and landform morphologies in a given location are the product of a complex system at the nexus of interrelated terrestrial, atmospheric, and—in coastal areas—aquatic processes (Schwarz et al., 2018). One of the “prime factors” controlling dune environments, according to Ritchie (1972), is climate. An indicator of environmental and climatic conditions controlling aeolian landscapes and dune geomorphic systems is often the development, presence, and modes of dune blowouts (Ritchie, 1972; Hesp, 2002). Blowouts are erosional depressions or troughs that have “blown out” through existing dunes due to natural or anthropogenic forcing (Bate and Ferguson, 1996; Hesp, 2002). The morphology of blowouts varies (Ritchie, 1972; Hesp and Hyde, 1996), as does the definition of the term “blowout” (Hesp and Hyde, 1996). Yet, blowout landforms generally include a deflation basin from which sand is eroded, lateral erosional walls that are often stabilized at their crests by vegetation, and a downwind depositional lobe onto which eroded sand is deposited (Adamson et al., 1988; Sloss et al., 2012).

Blowout initiation occurs due to an assortment of drivers, including wave and fluvial erosion, aeolian erosion from high-velocity winds and the aerodynamic influences associated with the topographic acceleration of airflow over a dune crest, the density of dune vegetation and its effectiveness at geomorphic stabilization, human and animal disturbance, storms, and changes in precipitation and temperature (Melton, 1940; Jungerius et al., 1981; Hesp and Hyde, 1996; Hesp, 2002; Jewell et al., 2017). Most of these initiation factors are related to climate, although the mechanisms are likely more complex than a simple climate-blowout coupling. After all, coastal dunes are complex systems involving interrelated process-response relationships and evolutionary drivers operating at different spatiotemporal scales (Delgado-Fernandez, 2011; Walker et al., 2017). For example, coastal dunes along Lake Michigan are the result of complex interactions among lake levels, climate, wind, vegetation, and littoral and dune geomorphic processes (Cowles, 1899; Olson, 1958a, b, c; Loope and Arbogast, 2000; van Dijk, 2004, 2014; Hansen et al., 2009; Walker et al., 2017; Fisher et al., 2021). Still, changes in climate invariably affect the sensitive ecogeomorphic feedbacks and relationships determining dune behavior and blowout mode in any dunefield (Thom et al., 1994).

Ecogeomorphic influence on dunes can be observed along Lake Michigan's shoreline, as White et al. (2019) and McKeehan and Arbogast (2021) suggest. Both studies observed an expansion in dune vegetation and, consequently, the geomorphic stabilization of some coastal dunes in the region in the modern era (White et al., 2019; McKeehan and Arbogast, 2021). Both speculated that an increase in precipitation in the last ca. 80 years was possibly driving the ecogeomorphic response observed across the landscape, although McKeehan and Arbogast (2021) also

provided other process-response explanations, including a non-linear ecogeomorphic lag from drier or stormier Holocene climates and potential anthropogenic forcing.

Driven by climatic forcing, it is ultimately the ecogeomorphic interactions at the dune scale where much variability exists (Melton, 1940; Hack, 1941; Cooper, 1958; Carter, 1991; McKenzie and Cooper, 2001; Hesp et al., 2011), creating the impetus for blowout formation. In illustrating this point, blowouts and parabolic dunes were observed to be “wind in conflict with vegetation” by Melton (1940, pp. 113–114), whereas Hack (1941, p. 242) described coastal dune geomorphologies as “a contest between moving sand and vegetation.” At areas of vegetative and topographic vulnerability, aeolian and other erosional processes undertake what Cooper (1958, p. 74) called the “concentration of effective attack by wind at a point of weakness,” resulting in the deflation of sand from the dune (Cooper, 1958; Schwarz et al., 2018). This creates “wind-scoured gaps” in individual dunes, leading to blowouts (Bagnold, 1941; Hesp, 2002). The effectiveness and consequence of the aeolian “attack” on a dune depends greatly upon the effective ecogeomorphic functionality of vegetation (Cooper, 1958; Ranwell, 1958; Gares, 1992; Gares and Nordstrom, 1995; Lancaster and Baas, 1998; Nield and Baas, 2008; Abhar et al., 2015; Schwarz et al., 2018; Lee et al., 2019; Miyanishi and Johnson, 2021). Weak, dead, or sparse vegetation may foster dune activation or blowouts (Schwarz et al., 2018). Further, vegetation and associated ecogeomorphic processes somewhat control blowout morphology post initiation (Gares, 1992).

Underscoring the interrelated ecogeomorphic processes at work in aeolian systems, the ample delivery of sand from beach and foredune areas windward of blowouts has many possible and varied outcomes on dunes and blowouts (Schwarz et al., 2018; Laporte-Fauret et al., 2021; Miyanishi and Johnson, 2021). For example, ample sand can bury and destroy existing vegetation, hamper attempts by pioneering species to become established, and provide the conditions by which adaptive dune plant species can thrive and stabilize dunes (Cowles, 1899; Olson, 1958b; Doing, 1985; Maun, 1998; Dech and Maun, 2005; Lane et al., 2008; Brown and Zinnert, 2018). Generally, sand supply is a key, dynamic variable controlling dunefield behavior and is related to beach width, active coastlines, dune morphology, and flow dynamics (Short and Hesp, 1982; Davidson-Arnott et al., 2018). Sand supply is also important to blowout development and is constrained or promulgated by interrelated ecogeomorphic and climatic factors at work in dune systems (Cooper, 1958). Ecogeomorphic feedback mechanisms foster favorable edaphic conditions or hinder pedogenesis and affect sand supply, thus either driving dune systems and blowouts toward stabilization regimes or activation. Pioneering plant species on vegetating dunes, for instance, are effective at deflecting and trapping airborne and saltating sediment. Consequently, this reduces the supply of sand downwind, grows the foredune, and enriches the soil in a positive ecogeomorphic feedback (Hesp, 1981, 1989; Maun, 1998; Gardner and McLaren, 1999; Werner et al., 2011; Ruggiero et al., 2018).

These interrelated ecogeomorphic processes, often in response to climatic and other disturbance forcings, also influence blowout morphology (Girardi and Davis, 2010; Schwarz et al., 2018). Cooper (1958) and Schwarz et al. (2018) both distilled blowout morphological types into the two primary forms: trough and saucer blowouts. Trough blowouts, as the name suggests, are characterized by a deep, elongated trench-like feature with high lateral walls, culminating in a depositional lobe several meters high

several meters downwind (Hesp, 2002). Additional geomorphic conditions for the development of trough blowouts include steep-sloped dunes and deep, sandy substrata (Hesp, 2002; Luo et al., 2019). Unsurprisingly, trough morphologies have been associated with high-velocity aerodynamic jets (Hesp and Hyde, 1996). Lake Michigan's coastal dunes contain many trough blowouts, including several exceeding 100 m in length.

Saucer blowouts are perhaps less dramatic on the landscape, appearing as a "shallow dish" often atop dunes or in environments with thin sand deposits (Hesp, 2002). Whereas trough blowouts often develop from strong onshore, unidirectional winds (Melton, 1940), saucer blowouts have been observed to be the product of winds perpendicular to blowout inception (Hails and Bennett, 1980). Hesp (2002) identified a third type of blowout morphology called cup blowouts but noted that these often were saucer blowouts that had evolved and deepened due to subsequent and continued erosion. Ritchie (1972) followed a different schema and identified five types of blowouts: cigar-shaped, V-shaped, scooped hollow, cauldron-and-corridor, and parabolic.

Importantly for our study, Ritchie (1972) classified parabolic dunes as blowouts. Many researchers prior to Ritchie (1972) and after have agreed that parabolic dunes—the classical U-shaped aeolian landform (Landsberg, 1956; Jennings, 1957)—are either blowouts (Melton, 1940; Bagnold, 1941; Hack, 1941; Cooper, 1958; Hansen et al., 2009), inextricably related to blowouts (e.g., Girardi and Davis, 2010), or represent an evolutionary stage of a blowout (Jungerius et al., 1981; McCann and Byrne, 1994). For example, Cooper (1958, p. 74) stated that a parabolic dune "is essentially a trough blowout." Bagnold (1941) viewed the entire parabola-blowout procession as a cycle in which a new dune was "born" downwind in the form of a depositional lobe, an idea with which Melton (1940) concurred under certain wind regimes. We agree with these analyses and include parabolic dune landforms in our assessment of Lake Michigan coastal blowouts.

In this paper, we attempt to identify all blowouts on the eastern shore of Lake Michigan within the State of Michigan, including those with parabolic morphologies in accordance with Cooper (1958) and others. We then conduct a series of spatiotemporal analyses to determine trends in blowout evolution. First, we utilized machine learning tools to map blowout extent using repeat aerial photography at separate timestamps: 1938, 1986–1988, and 2018. Then, in a manner similar to Abhar et al. (2015) in their study of coastal dune blowouts on Cape Cod, Massachusetts, we employed an object-based image analysis technique known as a spatial-temporal analysis of moving polygons (STAMP) model to assess whether the polygons representing blowouts expanded, migrated, stabilized, or fragmented. By examining the trends in blowout behavior since 1938, we may be able to determine if the dune stabilization trends observed by White et al. (2019) and McKeehan and Arbogast (2021) extend to these geomorphic markers of climatic and ecogeomorphic forcing. In discussing our results, we also ascribe possible drivers of the observed blowout trends and the implications for Lake Michigan's dune systems.

METHODOLOGIES

Aerial imagery

A time-series geomorphic analysis of sand dunes often employs repeat aerial imagery (e.g., Jungerius and van der Meulen, 1989;

Belford et al., 2014; Abhar et al., 2015; White et al., 2019). For our purposes, blowouts along Lake Michigan's eastern shore, including on islands in the northern part of the lake, were identified and their extent mapped by examining three sets of summer aerial imagery representing three distinct timestamps: 1938, 1986–1988, and 2018 (Table 1). Aerial imagery from 1938, the oldest available for the region, was captured by the U.S. Department of Agriculture (USDA) in an attempt to develop a scientifically driven New Deal conservation and land use planning program (Monmonier, 2002). Images from the same dataset were used by White et al. (2019) in their study of coastal dunes in Michigan state parks. We obtained hundreds of 1938 aerial images of Lake Michigan coastal dune areas from Michigan State University's Remote Sensing and GIS Aerial Imagery Archive. These images are black and white (BW) panchromatic with a scale of 1:20,000 and a post-georeferenced spatial resolution of ~0.8 m.

Aerial imagery for 1986–1988 was obtained from the U.S. Geological Survey's (USGS) National High Altitude Photography (NHAP) program dataset (EROS, 2018a), a dataset sometimes used for mid-1980s landscape analyses (Rango et al., 2008). This 1986–1988 dataset was selected due to its availability and to provide a rough midpoint between the oldest and most recent complete imagery sets. Studies have employed NHAP aerial imagery for analysis of forest stand landscapes (e.g., Goldmann, 1990) and to evaluate land use land cover (LULC) change over time (Drummond et al., 2019), among other analyses. For areas along the southern portions of the lakeshore, NHAP BW images from 1988 with a scale of 1:80,000 were used (EROS, 2018a), while farther north, no suitable NHAP images for the year 1988 were available. Thus, we used NHAP images from 1986 for analysis of these areas, which included the Leelanau Peninsula. Occasionally, BW images were not available, in which case NHAP color infrared (CIR) aerial photographs with a 1:58,000 scale were used instead. The spatial resolution of all NHAP imagery post-georeferencing was ~6 m.

For 2018 images, we used aerial photography from the National Agricultural Imagery Program (NAIP) dataset (EROS, 2018b). The NAIP dataset imagery, which was captured by the USDA during the growing season, has a spatial resolution of ~0.6 m and three spectral visible color bands: red, green, and blue. In similar studies, the scale was reported to be 1:20,000 (e.g., Abhar et al., 2015). The NAIP dataset, which was also obtained through the USGS, contains the highest spatial resolution among the three sets of imagery.

Blowout mapping

All blowout mapping tasks, with the exception of STAMP model analyses, utilized ArcGIS 10.7 software (ESRI, 2021). Imagery from the 1938 USDA and NHAP datasets required georeferencing, and the NAIP dataset was used as a base reference in this task. Ground control points (GCPs) visible on images at all three periods were used to effectuate rubbersheeting during the georeferencing process. The establishment of GCPs was often challenging because shorelines and dunefields in the Lake Michigan basin are dynamic environments subject to geomorphological changes (Theuerkauf et al., 2021). In more-developed areas, landmarks, lighthouses, and static street intersections, along with other built environment infrastructure, were used as GCPs, while in less-developed areas, GCPs were often sentinel trees, country crossroads, and old barns. Almost all georeferencing

Table 1. Spatial characteristics and uncertainty for aerial image datasets used in this study. Sources for this information include Abhar et al. (2015), EROS (2018a, b), and White et al. (2019); loosely based on Mathew et al. (2010) and Abhar et al. (2015). Uncertainty is estimated as the sum of the published horizontal accuracy, average root mean squared error (RMSE) from georeferencing, and 1, which represents the potential error from resampling and vectorization. Aerial imagery sources include the U.S. Department of Agriculture (USDA) and the U.S. Geological Survey's (USGS) National High Altitude Photography (NHAP) and National Agricultural Imagery Program (NAIP) datasets.

Year	Source	Scale	Spatial Extent	Pixel Resolution (m)	Horizontal Accuracy (m)	Average Georeferencing RMSE (m)	Total Estimated Uncertainty (m)
1938 (BW)	USDA	1:20,000	~4000 × 4000 m	~0.8	—	~1	~2
1986-1988 (BW)	NHAP	1:80,000	7.5' USGS quadrangle	~6	—	~3	~4
1986-1988 (CIR)	NHAP	1:58,000	7.5' USGS quadrangle	~6	—	~2	~3
2018 (Color)	NAIP	1:20,000	3.75' × 3.75' USGS quarter quadrangle	~0.6	~1	—	~2

attempts required either second-order or third-order polynomial transformations. The target total Root Mean Square Error (RMSE) for each georectification was <5 m and was often <1 m (Table 1), especially for the 1938 aerial images because they covered smaller, although irregular, geographic areas (~4000 × 4000 m). By contrast, each NHAP image comprises a 7.5-minute USGS quadrangle (EROS, 2018a).

The locations of blowout features were identified by examining the breadth of the shoreline within each aerial imagery dataset, informed by various Michigan dune databases and reports (e.g., Buckler, 1979; Paskus and Enander, 2019; Arbogast et al., 2020). However, the most influential guide to blowout identification for our purposes was the Michigan Coastal Dune geodatabase created by Michigan State University researchers and managed by the Michigan Department of Natural Resources (DNR) (Arbogast et al., 2018). This GIS data resource contains the polygonal extent of 93,249 hectares (230,423 acres) of coastal dunes within the state of Michigan, although it did not delineate blowouts (Arbogast et al., 2018). Blowout-like features on aerial images well outside the spatial extent of the Michigan Coastal Dune GIS data were not flagged for mapping and were ignored in our workflow. By relying on these reports and datasets, it is possible we committed commission and omission errors during this identification process. When in conflict, however, we sought to lower the instances of omission error rather than commission error. For example, as we stated in the Introduction section, we classified parabolic dunes as blowouts for this analysis. Moreover, we feel the inclusion in this study of parabolic dunes and some other transgressive dune landforms that exhibit blowout behavior is geomorphically sound and follows the approaches taken in other studies (e.g., Melton, 1940; Cooper, 1958).

This methodology also follows the approach of Buckler's (1979) mapping study of Lake Michigan's coastal dunes, which termed parabolic dunes "central extensions" of blowouts. Although we counted parabolic dunes and other transgressive dune features as blowouts, each site needed to meet criteria for inclusion in the study. Jungerius et al. (1981) noted that classic scour blowout morphology begins to manifest itself upon the landscape after initiation once the deflation basin reaches 5 m in length. Yet, such an identification criterion for this study would be impossible given the spatial resolution and uncertainty of our data. Therefore, we used a criterion noted in Hesp's (2002) survey, which observed that a 1:1 morphodynamic relationship between the length of a blowout's deflation basin and its depositional lobe begins at ~20 m of basin length. Smaller blowouts do not appear to share this morphodynamic relationship and, thus, call into question whether they could be accurately and consistently identified in aerial photos. Consequently, we adopted the 20 m deflation basin length as an identification criterion, while allowing some slightly smaller blowouts to be included if they were positively identified in our investigation.

The spatial extents of the blowouts we identified were then generated for each of the three timestamps of our spatiotemporal analysis. To accomplish this, we used machine learning (ML) techniques to map the blowout boundary by detecting bare sand in a way that minimized human bias. We first down-sampled the 1938 and 2018 aerial images to match the relatively coarser spatial resolution of the NHAP dataset in ArcGIS using the bilinear interpolation method. In a time-series analysis of landscapes, resampling finer-resolution raster datasets to match the coarsest resolution dataset is considered best practice (Campbell, 1996, p. 577). To not resample the higher-quality

imagery would inject an additional vector of error into the time-series analysis by comparing maps that “differ greatly in detail and accuracy” (Campbell, 1996, p. 577). After resampling, we selected an unsupervised ML algorithm known as the Iterative Self-Organizing Data Analysis Technique (ISODATA) method. The ISODATA classification method is often used in landscape analyses (e.g., Lemenkova, 2021), including in analyses of coastal environments (Tojo and Udo, 2018), due to its efficiency in processing large remote sensing datasets without the need for supervised training samples (Ma et al., 2020). Moreover, unsupervised ML methods, including the ISODATA algorithm, “offer the promise of objective anomaly assignment” (Kvamme et al., 2019, p. 313), thus potentially reducing the bias of the authors to guide these procedures (Campbell, 1996, p. 318). By contrast, supervised ML methods for identifying bare sand in coastal dunefields were found to have issues of repeatability (Smyth et al., 2022).

Our process sought to leverage the contrast between the high albedo of bare dune sand with the relatively lower albedo of vegetated dunes, in a manner similar to Belford et al.’s (2014) time-series analysis of three Lake Michigan coastal dunes using repeat aerial imagery. More specifically, because the ISODATA ML algorithm effectuates its classification of an image by clustering pixels into statistically alike bins, we expected that a high-albedo bare sand cluster would naturally emerge separately amid a large lake, mid-latitude temperate forests, and other vegetation and built structures. The ISODATA method runs multiple iterations, regrouping pixels into possible bins, recalculating their means, and assessing the effects on pixel organization before statistically determining pixel classification (Campbell, 1996, p. 337; Abbas et al., 2016; Ma et al., 2020). After using ArcGIS to generate a rasterized pixel cluster of bare sand at a blowout location, we converted the blowout raster to a vector polygon. Some feature editing was necessary to separate the blowout throat from Lake Michigan’s coastal foreshore, because this usually is not classified as part of a dune blowout. From this, we were able to create a geo-spatial inventory of coastal dune blowouts on Lake Michigan’s eastern shore at three timestamps beginning in 1938. We also calculated each blowout’s physical area, upwind orientation, and computed the amount of dune loss to human development, where applicable.

Assessing the accuracy and uncertainty of aerial image analyses of the environment is difficult given the numerous sources of error and lack of uniform standards in aerial imagery studies (Lunetta et al., 1991), especially in dynamic coastal areas (Moore, 2000; Smyth et al., 2022). Within our workflow, potential sources of error included the horizontal accuracy of the original photographs, the georeferencing process for the 1938 and 1986–1988 aerial images, the resampling of 1938 and 2018 aerial imagery, the ISODATA bare sand classification process, and the conversion of ISODATA rasterized results to vector polygons (Lunetta et al., 1991; Congalton, 1997; Moore, 2000; Mathew et al., 2010; Abhar et al., 2015). In addition to calculating the RMSE associated with the georeferencing process (see above), we estimated uncertainty (Table 1). Somewhat similar to Mathew et al. (2010) and Abhar et al. (2015), we calculated uncertainty by adding the published horizontal error from each aerial photo dataset, the RMSE generated after georeferencing, and estimated delineation error from resampling and vectorization. Our uncertainty values are in line with those reported by Mathew et al. (2010) and Abhar et al. (2015) and in most cases are within 1 m. This approach was adopted because our focus was bare sand

identification and changes in blowout morphology. Because this study sought only to identify bare sand, we did not calculate the error matrix typically associated with remote sensing land cover classification analyses (Foody, 2002). As such, we did not assess classification accuracy or generate user and producer error statistics.

To determine whether blowouts in 1938 differ statistically from blowouts in 2018, we used a Wilcoxon signed-ranks test. This test is the nonparametric equivalent of the paired samples *t*-test and was selected because we assumed the distribution of blowout size for both timestamps would be nonnormative (Wilcoxon, 1945; Corder and Foreman, 2009). The Wilcoxon signed-ranks test was designed to compare a set of two paired samples of data to determine if significant differences exist between the sets. To do this, blowouts were ranked based upon the absolute value of the difference between the values of each pair, which in this case was the blowout size in square meters for 1938 and 2018 (Corder and Foreman, 2009) (Equation 1). The sign difference is recorded, then all the number of positive ranks (ΣR_+) and negative ranks (ΣR_-) are summed separately (Corder and Foreman, 2009). The lesser of ΣR_+ and ΣR_- is the *T*-statistic, which is then fed into a formula to calculate the *Z*-statistic, a commonly used metric in trend analyses (Corder and Foreman, 2009; Gocic and Trajkovic, 2013):

$$Z = \frac{T - \bar{x}_T}{S_T} \quad (1)$$

where \bar{x}_T is the mean of the *T*-statistic and S_T is its standard deviation. In terms of aeolian geomorphology research, the Wilcoxon signed-ranks test was used recently in a study of soil differences in coastal sand dunes, although the specific *Z*-statistic results were not divulged (Lopez et al., 2020). We calculated the *Z*-statistic from the Wilcoxon signed-ranks test for blowout sizes using the Two-Related Samples tool in IBM SPSS Statistics 27 (IBM Corp., 2020). To isolate the statistical analysis from anthropogenic influences, we removed from the Wilcoxon signed-ranks test all blowouts where human development visibly contributed to blowout loss. We also removed all blowouts from the test that had any missing data for either 1938, 1986–1988, or 2018. Typically, the null hypothesis for a Wilcoxon signed-ranks test is that no differences exist between the 1938 and 2018 blowout sizes; our research hypothesis, however, was otherwise.

STAMP Model

Although time-series analyses of dune behavior using repeat aerial imagery is relatively common in aeolian geomorphology, the manner in which landscape change is assessed often diverges among studies. Scientists have used edge tracing over multiple images to study dune migration in Indiana on Lake Michigan southern shore (Kilibarda and Shillinglaw, 2015), geographic information system (GIS) edge detection methods for three dunes near Holland in Michigan (Belford et al., 2014), remote sensing surface classifications in France (Rapinel et al., 2014), and an object-oriented approach at Cape Cod (Abhar et al., 2015), among other techniques. Here, we utilized an object-based image analysis technique advanced by Abhar et al. (2015) in their study of coastal dune blowouts on Cape Cod in Massachusetts (USA). They employed a STAMP model, a process first proposed

by Sadahiro and Umemura (2001) and codified into a model by Robertson et al. (2007). A STAMP model attempts to measure and classify the spatial changes in objects over time by quantifying their topologies and movements (Sadahiro and Umemura, 2001; Robertson et al., 2007). Changes are measured quantitatively as the difference between T_1 and T_2 timestamps, and the change is then classified into categories, including “expansion,” “stable,” and “contraction” (Figure 2). From this, landform changes over time can be described. For our study, the STAMP model evaluated two types of time-transgressive events: (1) changes in two-dimensional (2-D) blowout morphology between 1938 and 1986–1988, and (2) changes in 2-D blowout morphology between 1986–1988 and 2018. Together, we predicted that analyses of these two events would yield possible mesoscale blowout behavioral trends, including possible blowout fragmentation. To run the STAMP model for all identified blowout locations, we utilized the R software package stamp (Long et al., 2018).

RESULTS

Blowout identification and characteristics

Our analysis identified 435 blowout features in 1938 along Lake Michigan’s eastern shore and on six islands: South Manitou, North Manitou, South Fox, North Fox, High, and Beaver (Figure 3, Table 2). Active blowouts accounted for at least $\sim 19.1\text{M m}^2$ or ~ 4700 acres in 1938, according to our analysis. By 2018, that number dropped to $\sim 12\text{M m}^2$ or ~ 3000 acres, consisting of a loss of $>7.1\text{M m}^2$ or 1700 acres since 1938—a decrease of $\sim 37\%$. Dune blowouts, however, represent a tiny proportion of the study area’s total aeolian landscape. Blowouts in 2018 accounted for just 2.9% of the $\sim 102,500$ acres of dunes along the eastern shore of Lake Michigan, based upon overall dunefield totals from the statewide dune database compiled as part of the Arbogast et al. (2018) study.

Spatially, Lake Michigan’s coastal dunes have been differentiated between dunefields north and south of the isostatic hinge line, which cuts across the lakeshore near Arcadia in northern Manistee County (Larsen, 1987; Lovis et al., 2012). Generally, north of the hinge line, large, perched dune complexes and progradational systems in embayments are more common, because ongoing isostatic rebound has a great influence on coastal and aeolian processes. By contrast, south of the hinge line, coasts are isostatically stable and dunes are influenced more by lake

level fluctuations (Lovis et al., 2012). Using this glacioisostatic spatial division of the lakeshore, there are 166 blowouts south of the hinge line and 269 blowouts in the isostatically active north. According to a volumetric analysis of the dunefields in the study area, less than half of the shoreline’s dune sand is north of the hinge line at Arcadia (Arbogast et al., 2009). Yet, the coastal regions north of Arcadia contain $\sim 62\%$ of the blowouts. Conversely, blowouts in the south lost more area overall (~ 1300 acres) and per blowout (~ 8 acres/site) than did blowouts in the north (~ 400 acres total, ~ 1.5 acres/site), despite having fewer blowouts. Spatially, Leelanau County, north of the hinge line and home to Sleeping Bear Dunes National Lakeshore, contains the largest number of blowouts with 116. Benzie County, just north of the hinge line and south of Leelanau County, has 90 blowouts, which is the second-highest total.

Some blowouts have disappeared. In 1938, Lake Michigan’s eastern shore and islands had 435 blowouts, but 37 of those had disappeared completely by 2018. Of those 37 blowouts, 35 disappeared due to human development. In all, 55 blowouts (12.6% of all 1938 blowouts) shrank in size partially or completely disappeared due to human development, primarily the construction of residential structures. Development accounted for a decrease of $\sim 1.4\text{M m}^2$ or ~ 350 acres in blowout extent between 1938 and 2018. Ottawa County lost by far the largest amount of blowout areas to development since 1938, losing $\sim 870,000\text{ m}^2$ or ~ 215 acres along its $\sim 40\text{-km}$ -long coast. This loss in Ottawa County is $>50\%$ of all blowout extent lost to human development in our study.

Although declines attributed to human development were an important component of blowout loss since 1938, most blowouts (313 or 72% of all blowouts) decreased in area due to the expansion of vegetation. In total, 368 blowouts (85%) contracted in size or disappeared from 1938 to 2018. Not all blowouts decreased in size or disappeared, however (e.g., 53 blowouts expanded since 1938, some greatly). The largest expansion in blowout size occurred in a Benzie County blowout in Crystal Lake Township off George Street; this blowout quadrupled in size over the 80-year time-series analysis. Mostly due to image quality issues, there was insufficient data to determine whether 14 blowouts expanded or contracted in size during the period in question. Regarding our analysis of blowouts at the 1986–1988 timestamp, we determined that blowouts had contracted at a higher rate over those ca. 50 years since 1938 (~ 25 acres/yr) than in the 30-year period between 1988 and 2018 (~ 16 acres/yr), exclusive of

Event Type STAMP name	Description	T_1	T_2	$T_1 \cup T_2$
Stable	Area of T_2 polygon that remains the same as T_1 polygon			
Contraction	Feature polygon contracts in area from T_1 to T_2			
Expansion	Feature polygon expands in area from T_1 to T_2			
Fragmentation*	Feature polygon contracts and expands in area from T_1 to T_2 and includes new polygons <small>*Not a defined STAMP model output, but an interpretation based on STAMP model literature</small>			

Figure 2. STAMP model event types used in our analysis (modified from Abhar et al., 2015). T_1 and T_2 represent feature extent at two different timestamps.

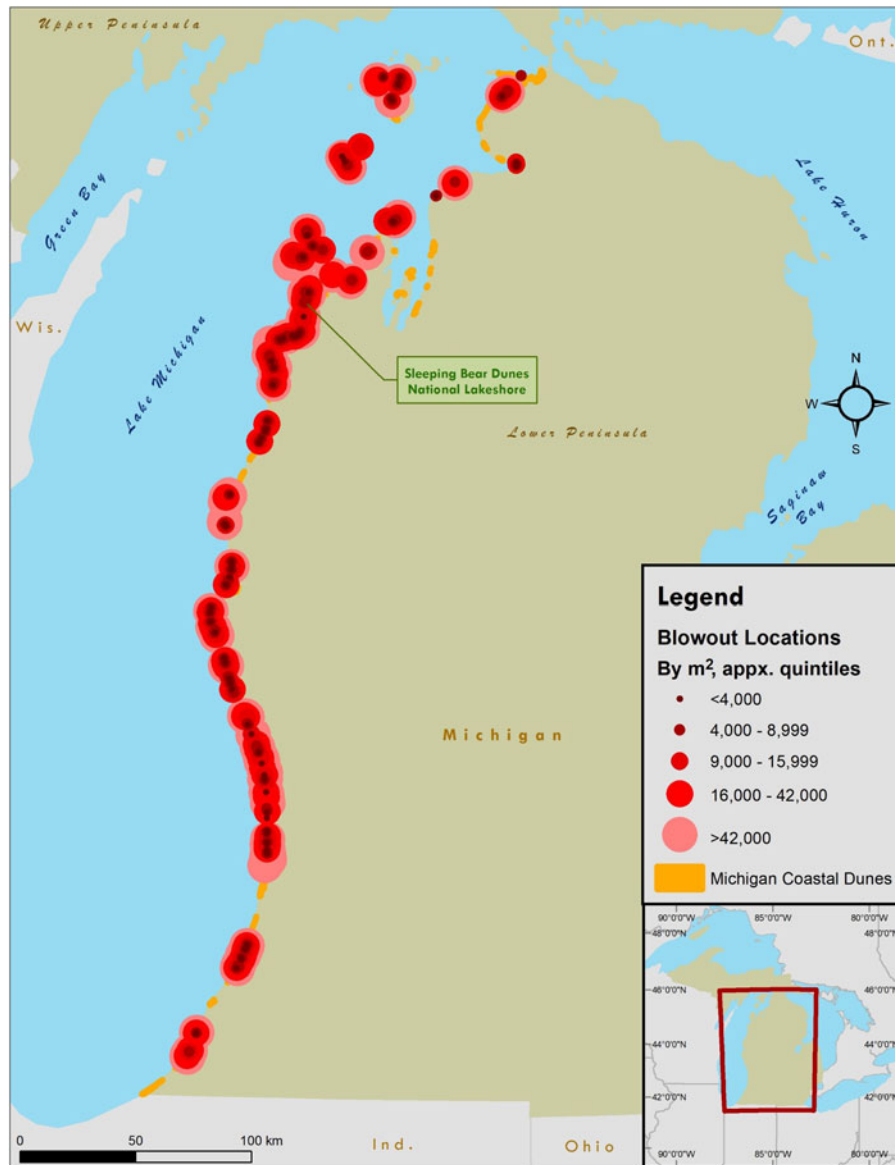


Figure 3. Blowout mapping results. Locations with 1938 spatial extent.

those affected by development, although we lacked data for 35 sites for the 1986–1988 timestamp.

According to the results of the Wilcoxon signed-ranks test, the differences in blowout extent between 1938 and 2018 are statistically significant (Table 3). The Z -statistic value of -13.526 exceeded the critical threshold, signifying significant differences between the two years. The Z -statistic is straightforward in its interpretation: the null hypothesis is rejected if $Z > \pm 1.96$ at the 5% significance level (Gocic and Trajkovic, 2013). Moreover, the sum of the negative ranks exceeded the positive ranks by a factor of 10, a condition that could be interpreted as a strong negative trend in blowout extent (Corder and Foreman, 2009).

Also importantly, we found no new blowouts since 1938, except small anthropogenically driven blowout-like features that occurred due to landscaping efforts at a handful of sites. These were not mapped or analyzed. However, the absence of new natural blowouts since 1938 potentially supports the findings that a negative trend in blowout activity is underway, as explained by the Wilcoxon signed-ranks test results. Additional analyses illuminated

geomorphic characteristics of the region's blowouts. For example, no relationship was found between magnitude of loss/gain in blowout extent and 1938 blowout size. In addition, both saucer and trough blowouts were found along the shore, but trough blowouts were more prominent (Table 4). However, the distribution of blowout type may be explained by geomorphic position. For example, several saucer blowouts were located on embayments, especially in the north (e.g., Platte Bay area south of Sleeping Bear). Positionally, most dunes are oriented perpendicular to the shore, with westerly orientations most common (Figure 4; Table 2).

STAMP Model

Fragmenting blowouts, examples of which can be seen in Figures 5 and 6, were observed in all sections of the shoreline through our analysis of the aerial images. Furthermore, the STAMP model determined that most blowouts, except those that had disappeared, both contracted significantly and expanded somewhat into new polygons, which can be interpreted partly as polygonal

Table 2. Blowout mapping results, organized geographically north to south. Some 1938 data are missing for Manistee County, thus the percentage change over time in blowout extent and computation of the loss due to human development there cannot be calculated completely. Some scattered totals may be incomplete for 1986–1988 for this reason, too. *Counties that contain islands with blowouts.

County	Blowouts	Total Blowout Extent (m ²) (×1000)			Percentage Change in Extent			Blowout Loss Due to Human Development			Mean Orientation
		1938	1986– 1988	2018	1938 to 1986–1988	1986 to 1988–2018	1938– 2018	Extent Loss (m ²) (×1000)	% of total loss	% of 1938 extent	
<i>North of hinge line</i>											
Emmet	31	616.2	472.2	353.6	–23.4%	–25.1%	–42.6%	61.7	23.4%	10.0%	W
Charlevoix*	32	547.2	464.4	366.1	–15.1%	–21.2%	–33.1%	2.0	1.1%	0.4%	WSW
Leelanau*	116	5233.7	4034.0	4312.0	–22.9%	+ 6.9%	–17.6%	0	0%	0%	WSW
Benzie	90	1778.5	1096.6	1445.2	–38.3%	+31.8%	–18.7%	0	0%	0%	W
<i>South of hinge line</i>											
Manistee	10	87.7	78.7	89.3	–10.3%	13.5%	+ 1.8%	18.0*	N/A*	N/A*	WNW
Mason	18	1461.3	626.5	585.0	–57.1%	– 6.6%	–60.0%	329.2	37.6%	22.5%	W
Oceana	23	923.4	638.8	432.1	–30.8%	–32.4%	–53.2%	15.4	3.1%	1.7%	W
Muskegon	34	1114.1	854.8	639.4	–23.3%	–25.2%	–42.6%	0	0%	0%	WSW
Ottawa	35	2325.1	1261.0	766.9	–45.8%	–39.2%	–67.0%	872.7	56.0%	37.5%	W
Allegan	16	3290.3	3048.1	1890.4	– 7.4%	–38.0%	–42.5%	33.4	2.4%	1.0%	W
Van Buren	18	489.3	481.8	222.2	– 1.5%	–53.9%	–54.6%	12.9	4.8%	2.6%	WNW
Berrien	12	1278.2	860.4	904.8	–32.7%	+5.2%	–29.2%	79.2	21.2%	6.2%	WNW
Total	435	19,145.0	13,917.4	12,007.0	–27.3%	–13.7%	–37.3%	1424.5	20.0%	7.4%	WNW

Table 3. Results of the Wilcoxon signed-ranks test. The null hypothesis is rejected if $Z > \pm 1.96$ at the 5% significance level (Gocic and Trajkovic, 2013). Thus, significant differences exist in the blowout extent from 1938 to 2018.

	n	Mean (m ²)	Std. Dev.		n	Sum of Ranks ΣR_+ or ΣR_-	T-statistic	Z-statistic	p-value (2-tailed)
1938 Blowout Extent	366	42,874.8	116,442.4	Negative Ranks	314	60,977			
2018 Blowout Extent	366	27,122.9	74,119.0	Positive Ranks	52	6184	6184	-13.526	<0.001

Table 4. Blowout morphology by type and county. The complex category represents blowout sites exhibiting both trough and saucer morphologies or locations that transitioned between morphologies since 1938. Some of these “complex” sites could best be categorized as fitting Ritchie’s (1972) “cauldron and corridor” morphology.

County	Total Blowouts	Trough	Saucer	Complex	Other/Undetermined
<i>North of hinge line</i>					
Emmet	31	18	7	4	2
Charlevoix	32	22	10	0	0
Leelanau	116	95	11	9	1
Benzie	90	54	27	7	2
<i>South of hinge line</i>					
Manistee	10	4	6	0	0
Mason	18	14	2	0	2
Oceana	23	12	9	2	0
Muskegon	34	24	8	0	2
Ottawa	35	22	8	5	0
Allegan	16	12	3	1	0
Van Buren	18	9	6	3	0
Berrien	12	7	3	2	0
Total	435	293	100	33	9

fragmentation (Robertson et al., 2007). Moreover, contraction, as measured by the STAMP model, was roughly twice the expansion of blowouts in 1986–1988 and 2018 (Fig. 7) (Long et al., 2018). Setting aside the photographic evidence from our aerial imagery analysis, it is unlikely that blowout contraction as measured by the STAMP model took place only at the polygonal boundaries of blowouts, given the 2:1 ratio of contraction to expansion. Instead, blowout fragmentation likely occurred to some degree within the previous extent of blowout polygons. In addition to blowout extent, the STAMP model also calculated the direction of blowout expansion, if any occurred. The results showed that some blowouts expanded downwind, even if the overall area of the blowout had decreased by 2018. Other blowouts prograded. Thus, no overall pattern of progression either leeward or windward was evident.

DISCUSSION

Our results show that most blowouts along the eastern shore of Lake Michigan have contracted in size since 1938, the starting point of our spatiotemporal analysis. Further, no new significant blowouts were detected at either the 1986–1988 or 2018 time-stamps, other than a handful of incidents tied directly to attempts at landscaping and terraforming windward of lakefront residential

properties. This fits a broad, global trend toward dune stabilization as observed in other studies (e.g., Gao et al., 2020), including the trend of vegetation expansion in European coastal dunes since 1900 (Provoost et al., 2011; Jackson et al., 2019a). Instead of expansion, most existing blowouts are not only contracting, but fragmenting, according to our analysis. Part of this broad reduction in blowout extent is the fragmentation of the bare sand areas of most blowouts, especially within their deflation basin, per the STAMP model results. Two questions emerge from these findings. First, what processes are driving this response by vegetation and blowouts? Second, if modern conditions are not conducive to blowout generation and expansion beyond the typical downwind expression of deflated sand onto the depositional lobe, then under what conditions did Lake Michigan’s coastal dune blowouts form?

Regarding the process-response formulation that is driving blowout fragmentation, our findings suggest that either sand supply has diminished, vegetation growth has accelerated beyond the threshold at which incoming sand can suppress it, or some combination of both processes. Lovis et al. (2012) speculated that the sand supply for Lake Michigan’s coastal dunes had decreased in the last 500 years. Sand supply to coastal dunes can be fostered or constrained by several interrelated variables, including those related to lake levels and wind. High water levels on Lake

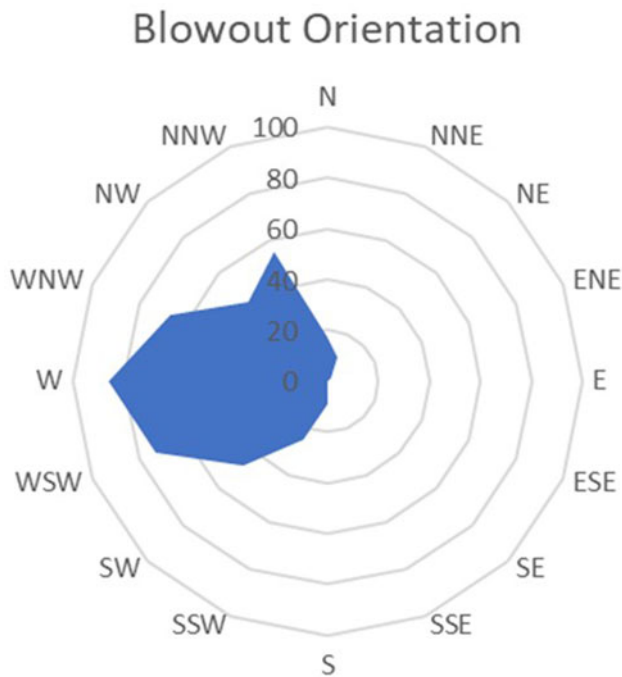


Figure 4. Blowout orientation, measured as the direction of the longitudinal axis of the blowout from its depositional lobe to its mouth. Thus, a blowout with a northerly orientation has its mouth north of its southerly depositional lobe and a north-south trending axis.

Michigan are related to dune activity and increased sand supply, according to several studies (Dow, 1937; Olson, 1958c; Anderton and Loope, 1995; Loope and Arbogast, 2000; Lovis et al., 2012). Mechanically, erosion of bluff sediment and beaches and the amount of foredune sand increase during periods of high lake levels, according to this model. Increased erosion feeds more sand into the coastal system, making it available for entrainment downwind into the dune system once delivered into the foreshore (Pye, 1983). The active transport of deflating or saltating sand through the dune system often simultaneously hampers vegetative growth and stimulates additional aeolian activity through landscape destabilization. Under these conditions in this model, the rate and manner of shoreline and beach retreat often are coupled with the rate of active inland dune migration—a geomorphic system state termed “beach negative; dune steady” by Sherman and Bauer (1993).

Yet, evidence also indicates the contrary. Nearshore, foreshore, and dune zones are coupled in complex ways that vary spatially and temporally, creating multiple possible “disequilibrium” and steady states (Sherman and Bauer, 1993). Importantly for this study, foreshore morphology, which is influenced by nearshore processes such as waves, swash, and longshore action (Salisbury, 1952; Short and Hesp, 1982; Short, 2012), affects the amount of sand supplied to the dune zone (Sherman and Bauer, 1993; van Dijk, 2004). Wide beaches, such as those possibly resulting from low levels on Lake Michigan, are associated with dissipative, yet high-energy, environments (Short and Hesp, 1982). Wide beaches

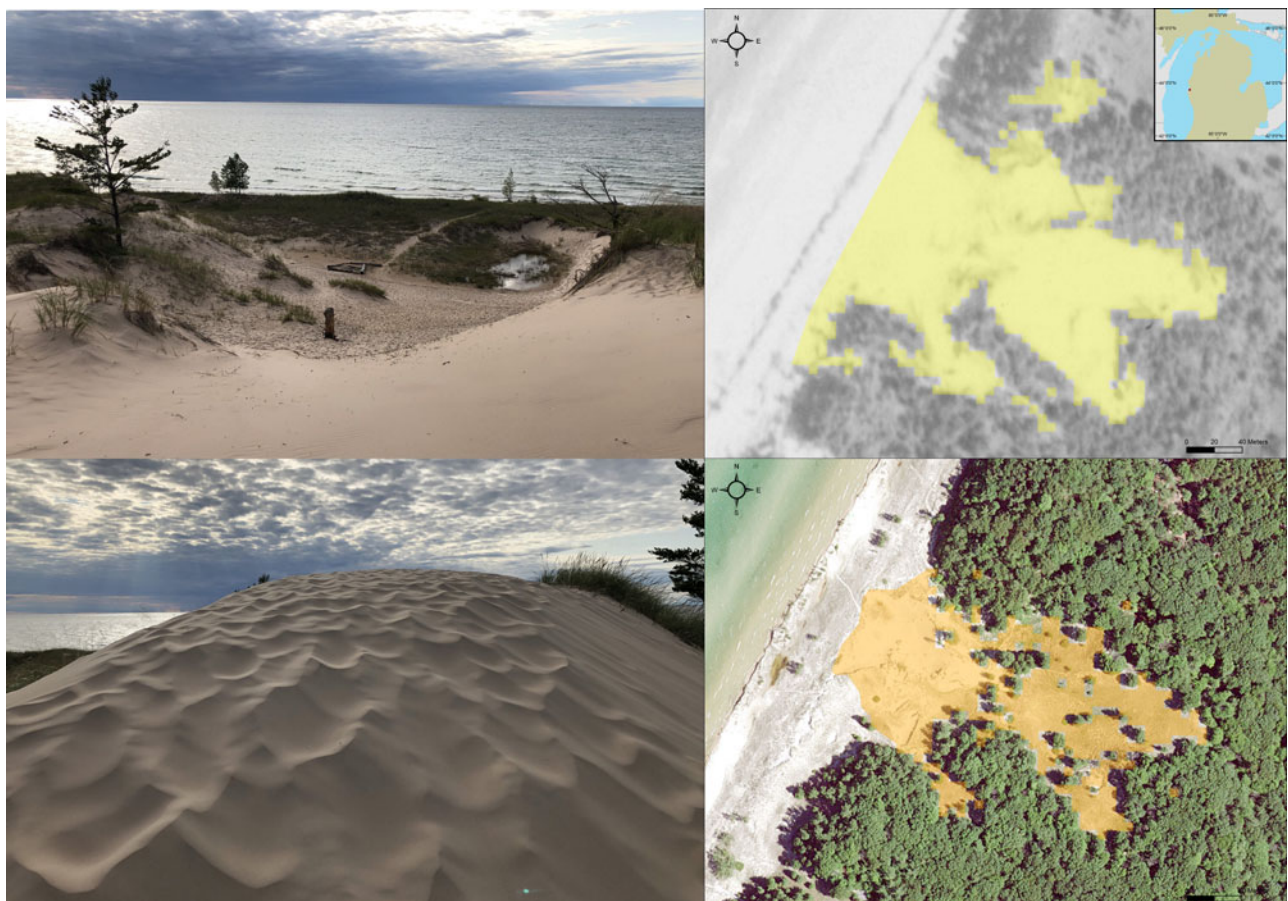


Figure 5. Blowout at Pentwater, Michigan, in Oceana County. On left, photographs from summer 2019 of the deflation basin (top) and depositional lobe (bottom). On right, blowout mapping results from 1938 (top) and 2018 (bottom). The 2018 results show fragmentation from sentinel trees and grasses. Ground-level photographs (left) taken by K.G. McKeenan.

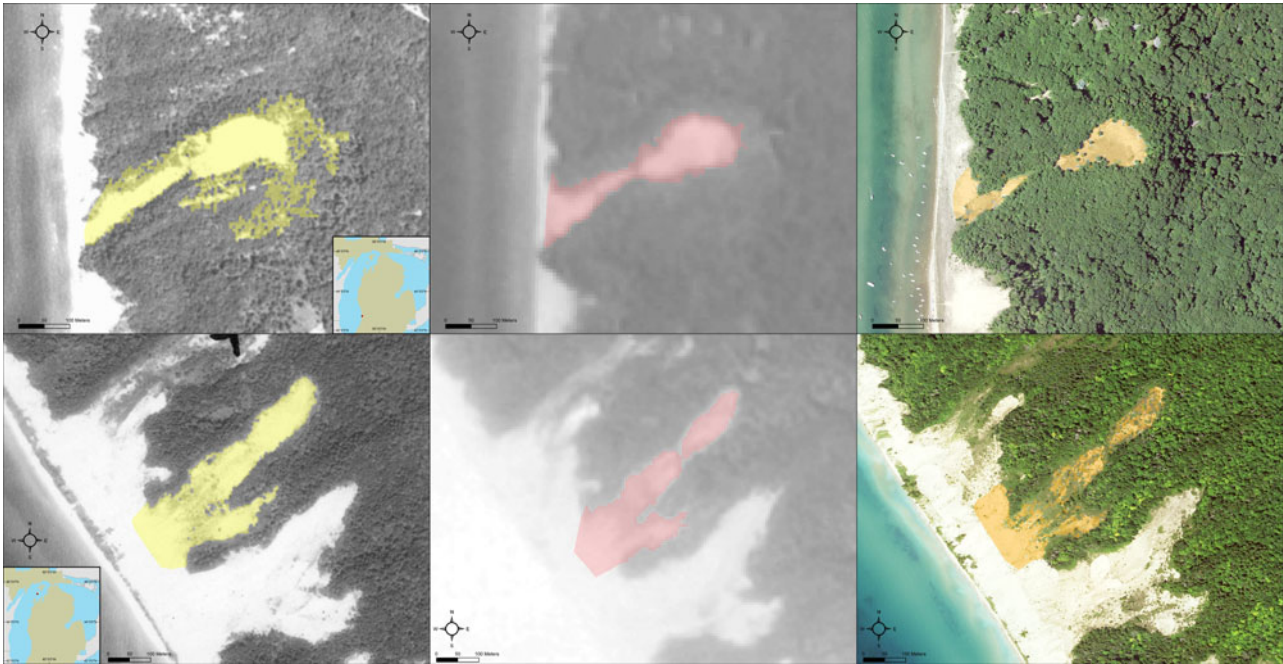
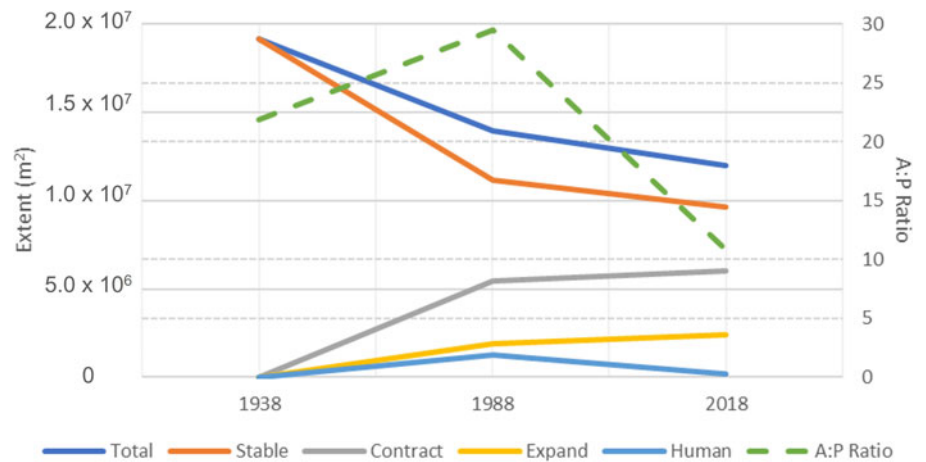


Figure 6. Examples of fragmentation of blowouts since 1938. Top row of images is from a blowout in Laketown Township, Michigan; bottom row of images is from South Fox Island in Lake Michigan. The images show the fragmentation of each blowout beginning in 1938 (left), 1986 (center), and 2018 (right).

Figure 7. STAMP analysis results. Each line tracks the trends in various STAMP categories from 1938 to 2018, including the area in m^2 determined to have remained within the blowout (Stable), the area lost within a blowout (Contract), and new blowout areas (Expand). Added to the figure are the areas associated with human development, the total blowout area, and the area-to-perimeter ratio (A:P) of each blowout polygon. The A:P ratio, a fractal geography metric, is interpreted here as a measure of fragmentation, as is the outpacing of contracted extent over expanded areas.



create the conditions for increased deposition of sediment on the foreshore and then the increased potential landward transport of sand due to the relatively longer fetch across the beach (Short and Hesp, 1982; Davidson-Arnott, 1988; Sherman and Bauer, 1993; Bauer and Davidson-Arnott, 2003; Delgado-Fernandez, 2010; Nordstrom, 2015; Hesp and Smyth, 2016). In an extensive study of coastal dunes at a state park in Michigan, van Dijk (2004) found that foredune growth occurred between 2000 and 2003 during a period of low lake levels and wide beaches at the study site. Fore dune growth did curtail sand supply to a dune rim downwind that was associated with a blowout (van Dijk, 2004), but such a circumstance seems to support the innate complexity of the process-response and ecogeomorphic mechanisms in coastal dune systems (Sherman and Bauer, 1993; Walker et al., 2017). Rather than driving all geomorphological components of the aeolian system in the state park into the same state, lower lake levels caused one response at the foredunes and another in the

backdunes (van Dijk, 2004), which underscores Carter's (1991) "natural heterogeneity" in dunefields. This bifurcated response echoes observations in dunefields elsewhere, either a cycled reworking or churning of dunes (e.g., Black, 1951; Dech et al., 2005), or even a state of "bistability" (e.g., Yizhaq et al., 2007).

Therefore, lake levels on Lake Michigan seem unlikely to be the primary driver of blowout state as outlined in our study. Both dune activity models involving lake levels are likely correct at any given time, but neither is predominant now. Over the course of our 80-year spatiotemporal study, Lake Michigan-Huron basin water levels fluctuated at a high frequency on roughly annual and decadal cycles around the modern mean (Bishop, 1990; Baedke and Thompson, 2000; Watras et al., 2014; Indiana DNR, 2020). Water levels can fluctuate as much as ~ 1 m annually in the extreme or up to almost 2 m over a decade, according to an analysis of historical data (Argyilan and Forman, 2003). There have been periods of both below- and

above-average lake levels (Theuerkauf et al., 2021), reflecting transient monthly, seasonal, annual, ca. 30-year, ca. 150-year, and other cycles that are sometimes evident during periods since the Nipissing high stand (Thompson and Baedke, 1997; Quinn, 2002; Argyilan and Forman, 2003; Watras et al., 2014). Moreover, since 2013, lake levels have been historically high (Indiana DNR, 2020; Theuerkauf et al., 2021). Yet, while lake levels fluctuate, no broad related trends exist that can explain blowout fragmentation or the lack of new blowouts. In other words, as Lake Michigan-Huron levels continue to cycle and change, albeit within a smaller range (Quinn, 2002), regional-scale blowout behavior has apparently decoupled—if it was ever coupled—from lake behavior and continued to trend toward fragmentation and stabilization at the impetus of vegetation expansion. Thus, other drivers likely are more influential.

An additional possible driver of decreased sand supply is a reduction in wind power. Some studies place wind power, or wind energy, at the forefront of dune behavior (e.g., Tsoar, 2005; Gunn et al., 2022), but other studies find it has less influence in aeolian landscapes than anticipated (e.g., Mason et al., 2008). Regardless, in coastal dunefields, the geomorphic function of wind includes transporting sand landward from the foreshore, a process involving a series of boundary layer adjustments (Walker et al., 2017). Deflating and saltating sand, along with the winds compelling these aeolian processes, interact with foreshore and dune topography, developing complex steering patterns and affecting dune surfaces and vegetation, among other features (Pluis, 1992; Arens, 1996; Bauer et al., 2012). As stated earlier, winds also can induce dune blowouts and guide their morphology (Melton, 1940; Cooper, 1958; Hesp, 2002; Schwarz et al., 2018).

Yet, determining wind energy as the primary driver stabilizing Lake Michigan's blowouts is difficult given the conflicting research results regionally and globally. Regionally, there is some evidence that wind energy may have declined as much as 40% along the eastern shoreline since 1960 (Yurk and Hansen, 2021), although there is also evidence that mean annual wind speed, drift potential, and other wind-influenced dune mobility indices, such as Lancaster's *M* (Lancaster and Helm, 2000), remained relatively unchanged over a similar period of time or declined slightly in the study area (McKeehan and Arbogast, 2021). Likewise, there is evidence that winds over various decadal time periods have decreased globally (Vautard et al., 2010; McVicar et al., 2012; Jackson et al., 2019a; Tian et al., 2019), increased over some oceans but decreased terrestrially (Torralba et al., 2017; Zeng et al., 2018), strengthened across Lake Superior to the north of our study area (Desai et al., 2009), and weakened across Minnesota to the northwest (Klink, 2002). Furthermore, the "stilling" of terrestrial winds, possibly due to the "greening" of land via expansion of vegetation (Zeng et al., 2018; Jackson et al., 2019a), that has been observed over the last several decades may be reversing (Zeng et al., 2019; Utrabo-Carazo et al., 2022).

In other words, no clear pattern with regards to wind energy has emerged yet in the Lake Michigan basin or anywhere else regionally. Moreover, wind data, whether from reanalysis or observational datasets, are often hampered by issues of completeness, error, and uncertainty (Julian, 1983; Morone, 1986; Torralba et al., 2017; Yin et al., 2021) and should be employed with caution. Given these mixed results, it is difficult to proclaim with certainty that a loss of wind energy across the study area is responsible for a reduction in sand supply in regional dunefields, although it could be a contributing variable.

A third factor in a potential regional reduction in sand supply is precipitation, which is a variable that has been identified in multiple dune models as a key control on vegetation (e.g., Ashkenazy et al., 2012; Delgado-Fernandez et al., 2019). Precipitation performs several ecogeomorphic functions in aeolian systems. Moist dune sand surfaces can increase the shear wind velocity threshold by which sand deflates, dampening aeolian erosion (Pluis, 1992; Cornelis and Gabriels, 2003; Han et al., 2011). Precipitation in the form of ice and snow has a chilling effect on wind erosion, as well (Doing, 1985; van Dijk, 2004, 2014). On the other hand, falling precipitation can also stimulate additional sand supply through splash erosion, which is the process by which sediment grains are knocked loose from the dune crust and made available for later wind entrainment (Jungerius and van der Meulen, 1988; Riksen and Goossens, 2007). Like most dune processes, even splash erosion is entangled with other variables in feedback mechanisms and process-response frameworks. For example, the effectiveness of splash erosion on dunefield sand supply depends upon the density of dune vegetation. If annual precipitation increases, the effectiveness of splash erosion might increase temporarily until soil moisture reaches a threshold at which vegetation coverage might increase as well, which in turn limits the effectiveness of splash erosion to affect sand supply.

Regardless, this description of splash erosion alludes to the main ecogeomorphic function of precipitation—the conduction of water into the sandy soil medium. As Tsoar (2005, p. 50) noted the "singular physical characteristic of the sandy soil" is the rapid delivery of water through the soil profile to the water table. Sand lacks the cohesion to hold water within its pores because the spaces between grains are relatively large (Salisbury, 1952; Dincer et al., 1974; Schaetzl and Anderson, 2005; Tsoar, 2005). This feature of sand is true regardless of the environment because both arid and humid sand dune soils share many key characteristics (Bar Kutiel et al., 2016). In other words, sand in a desert environment responds in a similar fashion to water as does coastal dune sand along Lake Michigan's eastern shoreline, which is a Udic soil moisture regime where precipitation is greater than potential evapotranspiration (PET) and dry conditions are rare (Schaetzl and Anderson, 2005).

Yet, if the amount of water supplied to a sand medium increases, pore spaces will become filled and moisture can be held, suggesting that each sandy soil may possess a threshold in the vadose zone by which water can be made available to plants (Sala et al., 1988; Gardner and McLaren, 1999). A relatively large increase in precipitation over time can have an accompanying, rapid response in vegetative growth in sandy soils (Sala et al., 1988; Ashkenazy et al., 2012). This process potentially sets in motion a series of ecogeomorphic feedback mechanisms. For example, dune sand soils holding more soil moisture due to an increase in annual precipitation and expansion of vegetation may demonstrate "temporal persistence" in soil moisture storage, according to the theory of the temporal stability of soil moisture (*TS SM*) (Vachaud et al., 1985; Wang et al., 2008). Persistently moist dune blowout soil may thus stay so, changing only in response to the needs of vegetation (Bar Kutiel et al., 2016). Further perpetuating these feedback mechanisms, organic matter and finer-grained particles are added to the soil as a consequence of vegetation growth, increasing water retention and supplying additional nutrients (Baldwin and Maun, 1983; Shay et al., 2000).

Importantly, vegetation is a notable control of blowout behavior. Upwind of the blowout and within the blowout itself,

vegetation can constrain sand supply to the blowout, essentially denying it nourishment. In a study of two dissimilar blowouts along New Jersey's coastline, Gares (1992) observed that vegetation had established itself in the throat of a blowout and had become the focal point for sand deposition, possibly growing into a foredune structure. This resulted in a "positive feedback that exists between vegetation growth and newly deposited sediment" (Gares, 1992, p. 602). A similar observation was made at a blowout in our study area near Petosky, Michigan, where a vegetated foredune starved a downwind blowout (Lepczyk and Arbogast, 2005).

Two recent studies have implied that vegetation growth in Lake Michigan's coastal dunes possibly may be ascribed to an increase in annual precipitation, among other possibilities (White et al., 2019; McKeehan and Arbogast, 2021). Annual precipitation increased ~180 mm since 1940 at two regional weather stations—South Bend, Indiana, and Muskegon, Michigan—along the southern and central portions of the lakeshore since 1940, but only modestly in the north at Traverse City (McKeehan and Arbogast, 2021). PET also has increased since 1940, but was still less than precipitation (McKeehan and Arbogast, 2021). Yet, a statistical analysis found these precipitation trends to be only moderately positive with respect to the southern and central coast. Thus, while an increase in annual precipitation is a possible driver of blowout contraction and fragmentation, especially given the rapid response of sandy soils to a sustained increase in water, we cannot be certain it is the primary process causing stabilization in the dune system. Instead, it is probable that multiple factors are at work, likely enmeshed in complex process-response relationships and ecogeomorphic feedback mechanisms (Schwarz et al., 2018; Delgado-Fernandez et al., 2019).

As we have mentioned, nearshore, beach, dune, and blowout processes in coastal systems are coupled through several interrelated variables that produce different outcomes in response to process stimuli, the results of which cycle feedback recursively throughout the system, changing the process-response relationships across spatiotemporal scales (Sherman and Bauer, 1993; Walker et al., 2017; Schwarz et al., 2018; Castelle et al., 2019; Delgado-Fernandez et al., 2019). A process-response framework of dune systems has been detailed in different ways in recent years (e.g., Ashkenazy et al., 2012; Delgado-Fernandez et al., 2019). Any understanding of the stabilization response by Lake Michigan coastal dunes would need to acknowledge a complex process-response framework, especially in the absence of a singular strong process driver trending toward obvious stabilization responses. After all, there are other potential drivers at work in the region, including increased atmospheric concentration of CO₂ through anthropogenic means, anthropogenically driven atmospheric nitrogen deposition, land use changes, fire suppression, the cessation of logging, and the growth of invasive species, all of which are discussed in McKeehan and Arbogast (2021) and Yurk and Hansen (2021).

One potential driver that likely has influenced blowout fragmentation, albeit at a localized scale, is the planting of grasses to stabilize active dunes. Beginning in the nineteenth century, some communities along Lake Michigan's eastern shoreline sought to minimize dust emissions and prevent the damage caused by drifting sand by planting grasses and trees atop bare sand dunes (Cowles, 1899; Sanford, 1916; Kroodsma, 1937; Lehotsky, 1972; Leege and Murphy, 2000, 2001; McKeehan and Arbogast, 2021). Planting campaigns occurred at multiple locations, including Saugatuck, Ottawa Beach near Holland, Grand

Haven, Muskegon, Pentwater, and Manistee, where two dunes known as "Maggie Thorpe" and "Creeping Joe" often caused problems for the community.

Importantly, however, the results of these efforts were mixed. For example, efforts to stabilize the dunes at Manistee and Saugatuck in 1902 by planting non-native black locust (*Robinia pseudoacacia*) and various spruces apparently succeeded upon inspection 12 years later in 1914 (Sanford, 1916). Yet, nearby efforts involving poplar trees and grasses failed, leaving stands of poplars half-buried in sand and no evidence that grasses had ever been present at the sites (Sanford, 1916). Other attempts, some led by then-Michigan Agricultural College (now Michigan State University), also failed to stabilize local dunes (Kroodsma, 1937). Yet, at Saugatuck in the 1930s, black locust and other tree species were used to stabilize dunes there successfully (Kroodsma, 1937). Consequently, similar tactics were employed using various pines to stabilize active dunes, which were a "menace" to nearby neighborhoods, at Grand Haven (Lehotsky, 1972). Later, 25,000 non-native Austrian pines (*Pinus nigra*) were planted in and around Saugatuck Dunes State Park from the 1950s to the 1970s in a mostly successful attempt to stabilize dunes (Leege and Murphy, 2000, 2001). In the late 1980s, grasses were used to stabilize a foredune fronting a housing development at Ottawa Beach (McKeehan and Arbogast, 2021).

From these examples, planting programs apparently have had a mixed record of success. They also have affected dune conditions at some, but certainly not all or even most, blowouts sites along Lake Michigan. Further, a thread of misconception that runs through some of these early planting studies is that the natural condition of Lake Michigan dunes is one in which the dunes are vegetated (e.g., Sanford, 1916; Kroodsma, 1937; Lehotsky, 1972), a theory made without the knowledge of regional dunefield geochronologies or features such as the Holland Paleosol. Sanford (1916) stated that logging and slash-and-burn clearing for agriculture were the culprits in reactivating stable dunes, while Lehotsky repeated the claim in 1972. However, McKeehan and Arbogast (2021) found this assumption to be untrue. Setting aside the regional aeolian geochronologies, an extensive examination by McKeehan and Arbogast (2021) of the U.S. General Office Public Lands Survey (PLS) notebooks in the state of Michigan's archives showed that bare sand dunes were common in the study area. These observations were made mostly prior to 1850 before widespread European settlement. Logging certainly occurred in some forested back dune areas, which were active thousands of years ago. Yet, the notebook evidence indicates the presence of progradational dune processes and long-term plant community succession, rather than logging and plantings being primary drivers of change on Lake Michigan's shoreline. Contrary to the findings of several early scientists, plantings were not returning Lake Michigan's coastal dunes to their natural tendencies; rather, the conditions of these dunefields are determined by multiple, multiscale process-response mechanisms. Planting success still likely hinged on favorable macroscale, mesoscale, and microscale climate and ecogeomorphic variables. Absent these favorable drivers, planting programs still could fail. The trees and grasses planted were still somewhat at the mercy of the vagaries of many factors, the most important being regional in scale. Planting programs, logging, and fire suppression are all pieces of the puzzle, but do not represent all or most of the puzzle.

It is worth noting that the most successful planting programs appear to have occurred after the drought of the 1930s. Naturally, improved techniques, ample funding, and scientific advances

could be responsible for the improved success of these programs. Yet, it is also possible that climatic or other factors drove these changes. Given the regional scale of blowout response, the most likely driver or combination of drivers of stabilization is uniform. Such drivers likely would be operating at meso- and macro-spatiotemporal scales, influencing local controls and feedbacks throughout the dune system, resulting in variability and heterogeneity of dune conditions at the scale of landforms and short temporal scales.

When answering questions of Lake Michigan coastal dune response, it may be helpful to think in terms of systems and states, despite some criticism of the ideas of landscape steady state or equilibrium (Thorn and Welford, 1994; Huggett, 2007, 2011). This theoretical approach has merit if the landscape system process-response scales and components are understood (Turner et al., 1993). For example, Sherman and Bauer (1993) developed a scheme that sought to classify nine types of beach-dune coupling and their associated ecogeomorphic environments, a framework that has been examined in other studies (Walker et al., 2017; Davidson-Arnott et al., 2018). In 2022, much of our study area would have been classified as “beach negative; dune positive” under this classification scheme, where high lake levels have encroached upon the beaches and made them less dissipative (Sherman and Bauer, 1993). At the same time, dune vegetation, which is expanding, is trapping sediment that ordinarily would be transported landward through the dune system, storing sediment, and creating a positive sediment budget.

Although compartmentalizing process-response environments might seem counterintuitive given the chaotic nature of outcomes in geomorphic systems (Phillips, 2006, 2007), these theoretic structures do provide the investigatory framework to begin detangling the complex ecogeomorphic feedbacks and mechanisms operating along Lake Michigan’s eastern shoreline. As a start, we can state that Lake Michigan coastal dune systems might be (1) driven toward a steady, vegetated state since the mid-Holocene; (2) driven between alternative states based upon which processes are dominant at a given scale; (3) in nonequilibrium due to a new process paradigm; or (4) responding chaotically to the same process stimuli (Phillips, 2007; Huggett, 2011). Further research would benefit from being designed with these geomorphic possibilities in mind.

One possible conceptual blowout model advanced here that incorporates this approach acknowledges three primary phenomenon—increased precipitation, fluctuating lake levels, and a trend toward “stillness,” as Zeng et al. (2018) and Jackson et al. (2019a) termed decreasing winds over land. Briefly, this model postulates that the moderate rise in annual precipitation has increased soil moisture across the study area and provided the pretext for growth of pioneering plant species, specifically species that do not require dune sand burial but are adapted to aeolian landscapes, such as eastern cottonwood (*Populus deltoides*) (Sanford, 1916). Increased moisture also dampens aeolian transport of sediment and fosters vegetation on foredunes, which is a critical ecogeomorphic marker for this model. Concurrently, during high lake level periods, transgressive lake action erodes some foredunes and bluffs, making sand available to the coastal dune system upon its eventual deposition onto the foreshore, if it is not lost offshore. During lower lake levels, the beach becomes dissipative, according to Short and Hesp’s (1982) model.

Conversely, the long fetch across the lake and higher energy allow for more efficient transport of sand from the foreshore into the backshore areas, stimulating foredune growth through

the ecogeomorphic capture of sediment, which creates a topographic barrier and blocks sand supply to downwind blowouts. This ecogeomorphic mechanism is key, especially in an environment of diminished wind power. Vegetation, which has pioneered inside the blowout deflation basin, thrives in the relatively high-precipitation, low-sand supply environment, enriching the soil through mutual feedback mechanisms and promoting additional vegetation growth. When transgressive lake behaviors return, the resultant high-stand foredune is somewhat eroded, partially removing the topographic barrier to the blowout and allowing for more sand to be supplied from the foreshore into the back-dune areas. Any bare or patchy sand areas receive additional sand supply; species adapted to sand burial, such as marram grass (*Ammophila breviligulata*) withstand this period and even bank seeds in the sand (Maun, 1998), especially if buried in <10 cm of sand (Zhan and Maun, 1994). With diminished wind power regionally, it’s possible that seeds are being buried by less sand than in years past, fostering higher rates of germination. Other fast-growing species, such as cottonwood trees, grow fast enough to outpace the rate of sand burial and survive. As lake levels fluctuate, the cycle begins again. A myriad of variables at the landform-scale, such as topographic position, local dune geomorphology, and human disturbance, among other factors, control some interactions and affect the overall state of blowouts in the dunefield.

If this represents a possible model to explain blowout contraction in the modern period, then under what conditions were blowouts along the eastern shore of Lake Michigan initiated and maintained, if current conditions largely are unfavorable for blowouts? Some evidence indicates that blowouts at the southern end of Lake Michigan at Indiana Dunes National Lakeshore originated during humid and cool periods (Kilibarda, 2018), although these observations were from foredune blowouts initiated by transgressive lake actions and storms. These blowouts then healed during subsequent low lake levels due to foredune growth, a similar mechanism observed by van Dijk (2004), suggesting an ephemeral temporal aspect to the observed blowouts in that study (Kilibarda, 2018). Our study did not detect these transitory blowouts, likely due to the relatively longer temporal design of our study. Yet, it is worth noting that blowouts were observed forming at the southern end of the lake during a time of high water levels, relatively higher humidity, and cool temperatures (Kilibarda, 2018). The most recent global cooling event was the Little Ice Age (LIA), a period roughly dated from ca. 0.7 ka to ca. 0.1 ka (Nordstrom, 2015) or ca. 1300–1900 AD. The LIA was a period of episodic dune activity in Europe (Provoost et al., 2011; Jackson et al., 2019b) and a period of cool, dry, and possibly erosive conditions around the Great Lakes (Colman et al., 2000; Hupy and Yansa, 2009; Warner et al., 2021), although lake levels appear to have been at or slightly above modern levels (Baedke and Thompson, 2000).

Could large, transgressive blowouts seen across the eastern shore of Lake Michigan be artifacts from the LIA period, which ended just as European settlement accelerated in the nineteenth century? It is possible, although it can be difficult to ascribe geomorphic events to specific climatic periods, especially since aeolian systems in general (Wright and Thom, 1977; Werner et al., 2011), and Lake Michigan’s coastal systems in particular (Lovis et al., 2012; McKeehan and Arbogast, 2021), can exhibit lagged responses to forcing. Still, optically stimulated luminescence (OSL) dates calculated from parabolic dune and blowout sand samples along the eastern shore of Lake Michigan show some

possible activity from the LIA. Fulop et al. (2019) reported one OSL date of 0.43 ± 0.05 ka from a parabolic dune at Green Point Dunes near Frankfort, while Lovis et al. (2012) reported a date of 0.62–0.76 ka at a blowout known as Mt. McSauba near Charlevoix. There is a smattering of other similar OSL dates associated with the LIA (Blumer et al., 2012; Lovis et al., 2012), but their association with parabolic dunes or blowouts is unclear. More dates exist linking dune and possible blowout activity to the Medieval Climate Optimum (MCO) (1.2–0.7 ka), the Roman Climate Optimum (RCO) (ca. 2.3–1.6 ka), and the Holocene Climate Optimum (HCO) (MIS 1). The oldest of these climatic intervals is the HCO, which in North America was the apogee of the mid-Holocene Northgrippian Age, a warm and dry period defined as ca. 8.2 ka to ca. 4.2 ka (Schaney et al., 2021) and sometimes referred to as the Hypsithermal (Warner et al., 2021). The HCO, which coincided with the Nipissing transgressions, was the period of origin for Lake Michigan's coastal dunes (Hansen et al., 2010), although it is unlikely that most blowouts would date to the HCO. As previously mentioned, periods of aeolian activity on the eastern lakeshore continued thereafter.

Interpreting OSL dates from other studies and applying them to speculative models of blowout behavior is difficult. Those studies were not designed with the goals of specifically establishing a theory of blowout development, nor do they provide a comprehensive picture of dunefield mode for the given time of activity or stability, considering Carter's (1991) "natural heterogeneity" and Yizhaq et al.'s (2007) "bistability." Yet, these studies do provide a baseline for our knowledge. According to these OSL dates, dune activity occurred at parabolic dune and blowout sites beginning at the HCO and in every other global warm period since then, with the exception of the current, anthropogenically driven warming period, which began in the late 1800s (Ruddiman, 2014, p. 391). Regardless, it is clear that many blowouts mapped in our study are relicts of the premodern environment, and that possibly some type of ecogeomorphic lag is underway in blowout response to Late Holocene conditions.

To resolve these questions, new research along the following two tracks would be helpful. First, to better understand why blowouts are healing, research should focus on determining which components of the process-response mechanisms are driving stabilization. New research could involve longitudinal studies in the field of key indicator blowouts to better understand geomorphic changes and drivers. Such research could attempt to determine regional blowout soil moisture thresholds, the process by which blowouts are vegetated, the effect of CO₂ and N on dune plants, how foredune growth affects blowout sand supply and fragmentation, how blowouts respond to human activity, especially in their deflation basins, and other component processes in the Lake Michigan dunes. The second important research track involves blowout geneses and the ecogeomorphic lag between initiation and fragmentation. For this research, it would be incumbent to date blowout inception, perhaps by concentrating on the depositional lobes of large trough blowouts. The designed research could incorporate spatial variability along the length of the lakeshore above and below the hinge line. Both research tracks are pertinent given the growing population of the region, economic value of the area, and the important dune ecosystems present (Harman and Arbogast, 2004; Schrottenboer and Arbogast, 2010; Arbogast et al., 2018, 2020). After all, although blowouts are currently stabilizing under vegetation, aeolian environments can experience rapid changes in short periods of time and are rarely stable for

long (Smith et al., 2017; Delgado-Fernandez et al., 2018; Miyanishi and Johnson, 2021).

CONCLUSIONS

In this time-series study, we mapped 435 dune blowouts along the eastern shore of Lake Michigan using repeat aerial photography, machine learning tools, and a STAMP model to quantify blowout behavior at three temporal periods. From 1938 to 2018, no new blowouts formed along the entire lakeshore. In addition, blowout extent decreased ~37%, primarily due to an expansion of vegetation, although human development played a significant role. Further, the STAMP model suggested that blowouts were not merely shrinking, but also fragmenting. This study confirmed the findings of White et al. (2019) and McKeehan and Arbogast (2021), who found that coastal dunes in the study area were stabilizing while vegetation was expanding over previously bare sand. The processes driving this response by blowouts are unclear but could be a series of interrelated factors that stimulate ecogeomorphic feedbacks. An increase in annual precipitation, lake level fluctuations, and a decrease in wind power may be affecting dune blowouts in complex ways at different spatiotemporal scales to drive stabilization. Further, because no new blowouts were detected in our study, we speculated that the conditions that initiated blowout formation have not occurred in the modern period and that blowouts in the study area may be geomorphic artifacts from climatic eras that were different than now, such as the Little Ice Age, Medieval Warm Period, and Roman Climatic Optimum. We also identified further research along two tracks that could resolve these questions. One track would investigate the process-response mechanisms that are driving blowout stabilization, while the other would explore blowout origins.

Acknowledgments. We gratefully acknowledge the Michigan State University (MSU) Department of Geography, Environment, and Spatial Sciences for their facilities and financial support. Additionally, we appreciate the staff of the MSU Remote Sensing and GIS (RS&GIS) group for their assistance navigating the university's Aerial Imagery Archive. We would also like to convey special thanks to Drs. Kyla Dahlin and Ethan Theuerkauf of MSU's Department of Geography, Environment, and Spatial Sciences, and Dr. Robert Richardson of the Department of Community Sustainability who reviewed early versions of this manuscript.

Disclaimer. Any use of trade, firm, or product names is for descriptive purposes only and does not imply endorsement by the U.S. Government.

REFERENCES

- Abbas, A.W., Minallh, N., Ahmad, N., Abid, S.A., Khan, M., 2016. K-means and ISODATA clustering algorithms for landcover classification using remote sensing. *Sindh University Research Journal (Science Series)* **48**, 315–318.
- Abhar, K.C., Walker, I.J., Hesp, P.A., Gares, P.A., 2015. Spatial-temporal evolution of aeolian blowout dunes at Cape Cod. *Geomorphology* **236**, 148–162.
- Adamson, D., Selkirk, P., Colhoun, E., 1988. Landforms of aeolian, tectonic and marine origin in the Bauer Bay-Sandy Bay region of subantarctic Macquarie Island. *Papers and Proceedings of the Royal Society of Tasmania* **122**, 65–82.
- Anderton, J.B., Loope, W.L., 1995. Buried soils in a perched dunefield as indicators of late Holocene lake-level change in the Lake Superior basin. *Quaternary Research* **44**, 190–199.
- Arbogast, A.F., Hansen, E.C., Van Oort, M.D., 2002. Reconstructing the geomorphic evolution of large coastal dunes along the southeastern shore of Lake Michigan. *Geomorphology* **46**, 241–255.

- Arbogast, A.F., Garmon, B., Sterrett Isely, E., Jarosz, J., Kreiger, A., Nicholls, S., Queen, C., Richardson, R.B., 2018. *Valuing Michigan's Coastal Dunes: GIS Information and Economic Data to Support Management Partnerships*. Michigan Environmental Council, Lansing, MI, 75 pp. https://www.environmentalcouncil.org/valuing_michigans_coastal_dunes.
- Arbogast, A.F., Schaetzl, R.J., Hupy, J.P., Hansen, E.C., 2004. The Holland Paleosol: an informal pedostratigraphic unit in the coastal dunes of south-eastern Lake Michigan. *Canadian Journal of Earth Sciences* **41**, 1385–1400.
- Arbogast, A.F., Shortridge, A.M., Bigsby, M.E., 2009. Volumetric estimates of coastal sand dunes in lower Michigan: explaining the geography of dune fields. *Physical Geography* **30**, 479–500.
- Arbogast, A.F., McKeehan, K.G., Richardson, R.B., Zimmnicki, T., 2020. *Learning to Live in Dynamic Dunes: Citizen Science and Participatory Modeling in the Service of Michigan Coastal Dune Decision-Making*. Michigan Environmental Council, Lansing, MI, 38 pp. https://www.environmentalcouncil.org/learning_to_live_in_dynamic_dunes.
- Arens, S.M., 1996. Patterns of sand transport on vegetated foredunes. *Geomorphology* **17**, 339–350.
- Argyilan, E.P., Forman, S.L., 2003. Lake level response to seasonal climatic variability in the Lake Michigan-Huron system from 1920 to 1995. *Journal of Great Lakes Research* **29**, 488–500.
- Ashkenazy, Y., Yizhaq, H., Tsoar, H., 2012. Sand dune mobility under climate change in the Kalahari and Australian deserts. *Climate Change* **112**, 901–923.
- Baedke, S.J., Thompson, T.A., 2000. A 4,700-year record of lake level and isostasy for Lake Michigan. *Journal of Great Lakes Research* **26**, 416–426.
- Bagnold, R.A., 1941. *The Physics of Blown Sand and Desert Dunes*. Methuen, London.
- Baldwin, K.A., Maun, M.A., 1983. Microenvironment of Lake Huron sand dunes. *Canadian Journal of Botany* **61**, 241–255.
- Bar Kutiel, P., Katz, O., Ziso-Cohen, V., Divinsky, I., Katra, I., 2016. Water availability in sand dunes and its implications for the distribution of *Artemisia monosperma*. *CATENA* **137**, 144–151.
- Bate, G., Ferguson, M., 1996. Blowouts in coastal foredunes. *Landscape and Urban Planning* **34**, 215–224.
- Bauer, B.O., Davidson-Arnott, R.G.D., 2003. A general framework for modeling sediment supply to coastal dunes including wind angle, beach geometry, and fetch effects. *Geomorphology* **49**, 89–108.
- Bauer, B.O., Davidson-Arnott, R.G.D., Walker, I.J., Hesp, P.A., Ollerhead, J., 2012. Wind direction and complex sediment transport response across a beach-dune system. *Earth Surface Processes and Landforms* **37**, 1661–1677.
- Belford, A., Kenbeek, S.D., VanHorn, J., van Dijk, D., 2014. Using remote sensing and geospatial analysis to understand changes to Lake Michigan dunes. In: Fisher, T.G., Hansen, E.C. (Eds.), *Coastline and Dune Evolution Along the Great Lakes*. *Geological Society of America Special Paper* **508**, 217–228.
- Bishop, C.T., 1990. Historical variation of water levels in lakes Erie and Michigan-Huron. *Journal of Great Lakes Research* **16**, 406–425.
- Black, R.F., 1951. Eolian deposits of Alaska. *ARCTIC* **4**, 89–111.
- Blumer, B.E., Arbogast, A.F., Forman, S.L., 2012. The OSL chronology of eolian sand deposition in a perched dune field along the northwestern shore of Lower Michigan. *Quaternary Research* **77**, 445–455.
- Brown, J.K., Zinnert, J.C., 2018. Mechanisms of surviving burial: dune grass interspecific differences drive resource allocation after sand deposition. *Ecosphere* **9**, e02162. <https://doi.org/10.1002/ecs2.2162>.
- Buckler, W.R., 1979. Dune type inventory and barrier dune classification study of Michigan's Lake Michigan shore. *Report of Investigation* **23**, Geological Survey Division, Michigan Department of Natural Resources, Lansing, MI, 14 pp.
- Campbell, J.B., 1996. *Introduction to Remote Sensing, 2nd ed.* The Guilford Press, New York, NY, 622 pp.
- Carter, R.W.G., 1991. Coastal dunes. In: Carter, R.W.G., *Coastal Environments: An Introduction to the Physical, Ecological, and Cultural Systems of the Coastlines*. Academic Press, London, pp. 301–354.
- Castelle, B., Marieu, V., Bujan, S., 2019. Alongshore-variable beach and dune changes on the timescales from days (storms) to decades along the rip-dominated beaches of the Gironde Coast, SW France. *Journal of Coastal Research Special Issue* **88**, 157–171.
- Colman, S.M., King, J.W., Jones, G.A., Reynolds, R.L., Bothner, M.H., 2000. Holocene and recent sediment accumulation rates in southern Lake Michigan. *Quaternary Science Reviews* **19**, 1563–1580.
- Congalton, R.G., 1997. Exploring and evaluation the consequences of vector-to-raster and raster-to-vector conversion. *Photogrammetric Engineering and Remote Sensing* **63**, 425–434.
- Cooper, W.S., 1958. Coastal sand dunes of Oregon and Washington. *Geological Society of America Memoir* **72**, 1–169.
- Corder, G.W., Foreman, D.I., 2009. *Nonparametric Statistics for Non-Statisticians*. John Wiley & Sons, Inc., Hoboken, NJ, USA, 247 pp.
- Cornelis, W.M., Gabriels, D., 2003. The effect of surface moisture on the entrainment of dune sand by wind: an evaluation of selected models. *Sedimentology* **50**, 771–790.
- Cowles, H.C., 1899. The ecological relations of the vegetation on the sand dunes of Lake Michigan: part I—geographical relations of the dune floras. *Botanical Gazette* **27**, 95–117.
- Davidson-Arnott, R., Hesp, P., Ollerhead, J., Walker, I., Bauer, B., Delgado-Fernandez, I., Smyth, T., 2018. Sediment budget controls on fore-dune height: comparing simulation model results with field data. *Earth Surface Processes and Landforms* **43**, 1798–1810.
- Davidson-Arnott, R.G.D., 1988. Temporal and spatial controls on beach/dune interaction, Long Point, Lake Erie. *Journal of Coastal Research* **3**, 131–136.
- Dech, J.P., Maun, M.A., 2005. Zonation of vegetation along a burial gradient on the leeward slopes of Lake Huron sand dunes. *Canadian Journal of Botany* **83**, 227–236.
- Dech, J.P., Maun, M.A., Pazner, M.I., 2005. Blowout dynamics on Lake Huron sand dunes: analysis of digital multispectral data from colour air photos. *CATENA* **60**, 165–180.
- Delgado-Fernandez, I., 2010. A review of the application of the fetch effect to modelling sand supply to coastal foredunes. *Aeolian Research* **2**, 61–70.
- Delgado-Fernandez, I., 2011. Meso-scale modelling of aeolian sediment input to coastal dunes. *Geomorphology* **130**, 230–243.
- Delgado-Fernandez, I., O'Keefe, N., Davidson-Arnott, R.G.D., 2019. Natural and human controls on dune vegetation cover and disturbance. *Science of the Total Environment* **672**, 643–656.
- Delgado-Fernandez, I., Smyth, T.A.G., Jackson, D.W.T., Smith, A.B., Davidson-Arnott, R.G.D., 2018. Event-Scale Dynamics of a Parabolic Dune and Its Relevance for Mesoscale Evolution. *Journal Geophysical Research Earth Surface* **123**, 3084–3100.
- Desai, A.R., Austin, J.A., Bennington, V., McKinley, G.A., 2009. Stronger winds over a large lake in response to weakening air-to-lake temperature gradient. *Nature Geoscience* **2**, 855–858.
- Dincer, T., Al-Mugrin, A., Zimmermann, U., 1974. Study of the infiltration and recharge through the sand dunes in arid zones with special reference to the stable isotopes and thermonuclear tritium. *Journal of Hydrology* **23**, 79–109.
- Doing, H., 1985. Coastal fore-dune zonation and succession in various parts of the world. *Vegetatio* **61**, 65–75.
- Dott, E.R., Mickelson, D., 1995. Lake Michigan water levels and the development of Holocene beach-ridge complexes at Two Rivers, Wisconsin: stratigraphic, geomorphic, and radiocarbon evidence. *Geological Society of America Bulletin* **107**, 286–296.
- Dow, K.W., 1937. The origin of perched dunes on the Manistee Moraine, Michigan. *Michigan Academy of Sciences, Arts, and Letters* **23**, 427–440.
- Drummond, M.A., Stier, M.P., Diffendorfer, J.E., 2019. Historical land use and land cover for assessing the northern Colorado Front Range urban landscape. *Journal of Maps* **15**, 89–93.
- EROS, 2018a. *USGS EROS Archive—Aerial Photography—National High Altitude Photography (NHAP)*. <https://doi.org/10.5066/F7M043NG>.
- EROS, 2018b. *USGS EROS Archive—Aerial Photography—National Agriculture Imagery Program (NAIP)*. <https://doi.org/10.5066/F7QN651G>.
- ESRI, 2021. *ArcGIS 10.7*. Environmental Systems Research Institute, Redlands, CA.
- Fisher, T.G., Weyer, K.A., Boudreau, A.M., Martin-Hayden, J.M., Krantz, D.E., Breckenridge, A., 2012. Constraining Holocene lake levels and coastal dune activity in the Lake Michigan basin. *Journal of Paleolimnology* **47**, 373–390.
- Fisher, T.G., DeVries-Zimmerman, S.J., Hansen, E.C., Wolin, J.A., Lepper, K., Spanbauer, T., 2021. Drought coincident with aeolian activity in a Great

- Lakes coastal dune setting during the Algoma Phase (3.1–2.4 ka), southwest Michigan. *Journal of Great Lakes Research* **47**, 1468–1484.
- Foody, G.M.**, 2002. Status of land cover classification accuracy assessment. *Remote Sensing of Environment* **80**, 185–201.
- Fulop, E.C.F., Johnson, B.G., Keen-Zebert, A.**, 2019. A geochronology-supported soil chronosequence for establishing the timing of shoreline parabolic dune stabilization. *CATENA* **178**, 232–243.
- Gao, J., Kennedy, D.M., Konlechner, T.M.**, 2020. Coastal dune mobility over the past century: a global review. *Progress in Physical Geography: Earth and Environment* **44**, 814–836.
- Gardner, R., McLaren, S.**, 1999. Infiltration and moisture movement in coastal sand dunes, Studland, Dorset, U.K.: preliminary results. *Journal of Coastal Research* **15**, 936–949.
- Gares, P.A.**, 1992. Topographic changes associated with coastal dune blowouts at island beach state park, New Jersey. *Earth Surface Processes and Landforms* **17**, 589–604.
- Gares, P.A., Nordstrom, K.F.**, 1995. A cyclic model of foredune blowout evolution for a leeward coast: Island Beach, New Jersey. *Annals of the Association of American Geographers* **85**, 1–20.
- Girardi, J.D., Davis, D.M.**, 2010. Parabolic dune reactivation and migration at Napeague, NY, USA: insights from aerial and GPR imagery. *Geomorphology* **114**, 530–541.
- Gocic, M., Trajkovic, S.**, 2013. Analysis of changes in meteorological variables using Mann-Kendall and Sen's slope estimator statistical tests in Serbia. *Global and Planetary Change* **100**, 172–182.
- Goldmann, R.A.**, 1990. *Using Multiresolution Remote Sensing Data and GIS Technology to Update Forest Stand Compartment Maps Under Lake States Conditions*. MS thesis, Department of Forestry, University of Wisconsin-Madison, Madison, WI.
- Gunn, A., East, A., Jerolmack, D.J.**, 2022. 21st-century stagnation in unvegetated sand-sea activity. *Nature Communications* **13**, 3670. <https://doi.org/10.1038/s41467-022-31123-8>.
- Hack, J.T.**, 1941. Dunes of the Western Navajo Country. *Geographical Review* **31**, 240–263.
- Hails, J.R., Bennett, J.**, 1980. Wind and Sediment Movement in Coastal Dune Areas. In: Edge, B.L. (Ed.), *Coastal Engineering 1980. Proceedings of the 17th International Conference on Coastal Engineering, held in Sydney, Australia, March 23–28, 1980*. American Society of Civil Engineers, New York, NY, pp. 1565–1575.
- Han, Q., Qu, J., Liao, K., Zhu, S., Zhang, K., Zu, R., Niu, Q.**, 2011. A wind tunnel study of aeolian sand transport on a wetted sand surface using sands from tropical humid coastal southern China. *Environmental Earth Sciences* **64**, 1375–1385.
- Hansel, A.K., Mickelson, D.M.**, 1988. A reevaluation of the timing and causes of high lake phases in the Lake Michigan Basin. *Quaternary Research* **29**, 113–128.
- Hansen, E.C., Arbogast, A.F., Packman, S.C., Hansen, B.**, 2002. Post-Nipissing origin of a backdune complex along the southeastern shore of Lake Michigan. *Physical Geography* **23**, 233–244.
- Hansen, E.C., Arbogast, A.F., van Dijk, D., Yurk, B.**, 2006. Growth and migration of parabolic dunes along the southeastern coast of Lake Michigan. *Journal of Coastal Research, Special Issue* **39**, 209–214.
- Hansen, E., DeVries-Zimmerman, S., van Dijk, D., Yurk, B.**, 2009. Patterns of wind flow and aeolian deposition on a parabolic dune on the southeastern shore of Lake Michigan. *Geomorphology* **105**, 147–157.
- Hansen, E.C., Fisher, T.G., Arbogast, A.F., Bateman, M.D.**, 2010. Geomorphic history of low-perched, transgressive dune complexes along the southeastern shore of Lake Michigan. *Aeolian Research* **1**, 111–127.
- Harman, J.R., Arbogast, A.F.**, 2004. Environmental ethics and coastal dunes in western Lower Michigan: developing a rationale for ecosystem preservation. *Annals of the American Association of Geographers* **94**, 23–36.
- Hesp, P.A.**, 1981. The Formation of Shadow Dunes. *Journal of Sedimentary Research* **51**, 101–112.
- Hesp, P.**, 2002. Foredunes and blowouts: initiation, geomorphology and dynamics. *Geomorphology* **48**, 245–268.
- Hesp, P.A.**, 1989. A review of biological and geomorphological processes involved in the initiation and development of incipient foredunes. *Proceedings of the Royal Society of Edinburgh, Section B: Biological Sciences* **96**, 181–201.
- Hesp, P.A., Hyde, R.**, 1996. Flow dynamics and geomorphology of a trough blowout. *Sedimentology* **43**, 505–525.
- Hesp, P.A., Smyth, T.A.G.**, 2016. Surfzone-Beach-Dune interactions: flow and sediment transport across the intertidal beach and backshore. In: Vila-Concejo, A., Bruce, E., Kennedy, D.M., McCarroll, R.J. (Eds.), *Proceedings of the 14th International Coastal Symposium* (Sydney, Australia). *Journal of Coastal Research, Special Issue* **75**, 8–12.
- Hesp, P., Martinez, M., da Silva, G.M., Rodriguez-Revelo, N., Gutierrez, E., Humanes, A., Láinez, D., et al.**, 2011. Transgressive dunefield landforms and vegetation associations, Doña Juana, Veracruz, Mexico. *Earth Surface Processes and Landforms* **36**, 285–295.
- Huggett, R.**, 2007. A history of the systems approach in geomorphology. *Geomorphologie Relief, Processus, Environnement* **13**, 145–158.
- Huggett, R.J.**, 2011. *Fundamentals of Geomorphology, Third Ed.* Routledge, London, New York.
- Hupy, C.M., Yansa, C.H.**, 2009. Late Holocene vegetation history of the forest tension zone in central Lower Michigan, USA. *Physical Geography* **30**, 205–235.
- IBM Corp.**, 2020. *IBM SPSS Statistics for Windows, Version 27.0*. Armonk, NY.
- Indiana DNR**, 2020. *Great Lakes Water Level Table for Lake Michigan/Huron*. Indiana Department of Natural Resources, Indianapolis, IN. <https://www.in.gov/dnr/water/files/03WaterLevelTable1981-2023LakeMichigan.pdf>.
- Jackson, D.W.T., Costas, S., González-Villanueva, R., Cooper, A.**, 2019a. A global 'greening' of coastal dunes: an integrated consequence of climate change? *Global and Planetary Change* **182**, 103026. <https://doi.org/10.1016/j.gloplacha.2019.103026>.
- Jackson, D.W.T., Costas, S., Guisado-Pintado, E.**, 2019b. Large-scale transgressive coastal dune behaviour in Europe during the Little Ice Age. *Global and Planetary Change* **175**, 82–91.
- Jennings, J.N.**, 1957. On the orientation of parabolic or U-dunes. *The Geographical Journal* **123**, 474–480.
- Jewell, M., Houser, C., Trimble, S.**, 2017. Phases of blowout initiation and stabilization on Padre Island revealed through ground-penetrating radar and remotely sensed imagery. *Physical Geography* **38**, 556–577.
- Julian, P.R.**, 1983. On the use of observation error data in FGGE main level III b analysis. ECMWF (European Centre for Medium-range Weather Forecasts) *Technical Memorandum* **76**. Shinfield Park, Reading, UK. <https://www.ecmwf.int/en/elibrary/75087-use-observation-error-data-fgge-main-level-iii-b-analysis>.
- Jungerius, P.D., van der Meulen, F.**, 1988. Erosion processes in a dune landscape along the Dutch coast. *CATENA* **15**, 217–228.
- Jungerius, P.D., van der Meulen, F.**, 1989. The development of dune blowouts, as measured with erosion pins and sequential air photos. *CATENA* **16**, 369–376.
- Jungerius, P.D., Verheggen, A.J.T., Wiggers, A.J.**, 1981. The development of blowouts in 'de blink', a coastal dune area near Noordwijkerhout, The Netherlands. *Earth Surface Processes and Landforms* **6**, 375–396.
- Kilibarda, Z.**, 2018. Humid and cool climate rather than droughts lead to coastal blowouts development in the Great Lakes region. *Geological Society of America Abstracts with Programs* **50**. <https://doi.org/10.1130/abs/2018AM-320964>.
- Kilibarda, Z., Shillinglaw, C.**, 2015. A 70-year history of coastal dune migration and beach erosion along the southern shore of Lake Michigan. *Aeolian Research* **17**, 263–273.
- Kilibarda, Z., Venturelli, R., Goble, R.**, 2014. Late Holocene dune development and shift in dune-building winds along southern Lake Michigan. In: Fisher, T.G., Hansen, E.C. (Eds.), *Coastline and Dune Evolution Along the Great Lakes*. *Geological Society of America Special Paper* **508**, 47–64.
- Kincare, K.A.**, 2007. Response of the St. Joseph River to lake level changes during the last 12,000 years in the Lake Michigan basin. *Journal of Paleolimnology* **37**, 383–394.
- Klink, K.**, 2002. Trends and interannual variability of wind speed distributions in Minnesota. *Journal of Climate* **15**, 3311–3317.
- Kroodsmas, R.F.**, 1937. The permanent fixation of sand dunes in Michigan. *Journal of Forestry* **35**, 365–371.
- Kvamme, K.L., Ernenwein, E.G., Menzer, J.G.**, 2019. Putting it all together: Geophysical data integration. In: Persico, R., Piro, S., Linford, N. (Eds.),

- Innovation in Near-Surface Geophysics: Instrumentation, Application, and Data Processing Methods*. Elsevier, Amsterdam, pp. 287–339.
- Lancaster, N., Baas, A.**, 1998. Influence of vegetation cover on sand transport by wind: field studies at Owens Lake, California. *Earth Surface Processes and Landforms* **23**, 69–82.
- Lancaster, N., Helm, P.**, 2000. A test of a climatic index of dune mobility using measurements from the southwestern United States. *Earth Surface Processes and Landforms* **25**, 197–207.
- Landsberg, S.Y.**, 1956. The orientation of dunes in Britain and Denmark in relation to wind. *The Geographical Journal* **122**, 176–189.
- Lane, C., Wright, S.J., Roncal, J., Maschinski, J.**, 2008. Characterizing environmental gradients and their influence on vegetation zonation in a subtropical coastal sand dune system. *Journal of Coastal Research, Special Issue* **24**, 213–224.
- Laporte-Fauret, Q., Castelle, B., Michalet, R., Marieu, V., Bujan, S., Rosebery, D.**, 2021. Morphological and ecological responses of a managed coastal sand dune to experimental notches. *Science of the Total Environment* **782**, 146813. <https://doi.org/10.1016/j.scitotenv.2021.146813>
- Larsen, C.E.**, 1987. Geological history of Glacial Lake Algonquin and the Upper Great Lakes. *U.S. Geological Survey Bulletin* **1801**, 1–36.
- Lee, D.B., Ferdowsi, B., Jerolmack, D.J.**, 2019. The imprint of vegetation on desert dune dynamics. *Geophysical Research Letters* **46**, 12041–12048.
- Leege, L.M., Murphy, P.G.**, 2000. Growth of the non-native *Pinus nigra* in four habitats on the sand dunes of Lake Michigan. *Forest Ecology and Management* **126**, 191–200.
- Leege, L.M., Murphy, P.G.**, 2001. Ecological effects of the non-native *Pinus nigra* on sand dune communities. *Canadian Journal of Botany* **79**, 429–437.
- Lehotsky, K.**, 1972. Sand dune fixation in Michigan—thirty years later. *Journal of Forestry* **70**, 155–160.
- Lemenkova, P.**, 2021. ISO Cluster classifier by ArcGIS for unsupervised classification of the Landsat TM image of Reykjavik. *Bulletin of Natural Sciences Research* **11**, 29–37.
- Lepczyk, X.C., Arbogast, A.F.**, 2005. Geomorphic history of dunes at Petoskey State Park, Petoskey, Michigan. *Journal of Coastal Research* **212**, 231–241.
- Lewis, C.F.M.**, 1969. Late Quaternary history of lake levels in the Huron and Erie basins. In: *Proceedings of the 12th Conference on Great Lakes Research, May 5–7, 1969, Ann Arbor, Michigan*. The University of Michigan and U.S. Bureau of Commercial Fisheries, pp. 250–270.
- Long, J., Robertson, C., Nelson, T.**, 2018. stamp: spatial-temporal analysis of moving polygons in R. *Journal of Statistical Software* **84**. <https://doi.org/10.18637/jss.v084.c01>.
- Loope, W.L., Arbogast, A.F.**, 2000. Dominance of an ~150-year cycle of sand-supply change in Late Holocene dune-building along the eastern shore of Lake Michigan. *Quaternary Research* **54**, 414–422.
- Lopez, O.M., Hegy, M.C., Missimer, T.M.**, 2020. Statistical comparisons of grain size characteristics, hydraulic conductivity, and porosity of barchan desert dunes to coastal dunes. *Aeolian Research* **43**, 100576. <https://doi.org/10.1016/j.aeolia.2020.100576>.
- Lovis, W.A., Arbogast, A.F., Monaghan, G.W.**, 2012. *The Geoarchaeology of Lake Michigan Coastal Dunes*. Michigan State University Press, East Lansing, MI, 252 pp.
- Lunetta, R.S., Congalton, R.G., Fenstermaker, L.K., Jensen, J.R., McGwire, K.C., Tinney, L.R.**, 1991. Remote sensing and geographic information system data integration: error sources and research issues. *Photogrammetric Engineering & Remote Sensing* **57**, 677–687.
- Luo, W., Wang, Z., Shao, M., Lu, J., Qian, G., Dong, Z., Hesp, P.A., Bateman, M.D.**, 2019. Historical evolution and controls on mega-blowouts in northeastern Qinghai-Tibetan Plateau, China. *Geomorphology* **329**, 17–31.
- Ma, Z., Liu, Z., Zhao, Y., Zhang, L., Liu, D., Ren, T., Zhang, X., Li, S.**, 2020. An unsupervised crop classification method based on principal components isometric binning. *ISPRS International Journal of Geo-Information* **9**, 648. <https://doi.org/10.3390/ijgi9110648>
- Mason, J.A., Swinehart, J.B., Lu, H., Miao, X., Cha, P., Zhou, Y.**, 2008. Limited change in dune mobility in response to a large decrease in wind power in semi-arid northern China since the 1970s. *Geomorphology* **102**, 351–363.
- Mathew, S., Davidson-Arnott, R.G.D., Ollerhead, J.**, 2010. Evolution of a beach-dune system following a catastrophic storm overwash event: Greenwich Dunes, Prince Edward Island, 1936–2005. *Canadian Journal of Earth Sciences* **47**, 273–290.
- Maun, M.A.**, 1998. Adaptations of plants to burial in coastal sand dunes. *Canadian Journal of Botany* **76**, 713–738.
- McCann, S.B., Byrne, M.L.**, 1994. Dune morphology and the evolution of Sable Island, Nova Scotia, in historic times. *Physical Geography* **15**, 342–357.
- McKeehan, K.G., Arbogast, A.F.**, 2021. Repeat photography of Lake Michigan coastal dunes: expansion of vegetation since 1900 and possible drivers. *Journal of Great Lakes Research* **47**, 1518–1537.
- Mckenzie, G., Cooper, A.G.**, 2001. Post emplacement dune evolution of Atlantic coastal dunes, Northwest Ireland. *Journal of Coastal Research, Special Issue* **34**, 602–610.
- McVicar, T.R., Roderick, M.L., Donohue, R.J., Li, L.T., Van Niel, T.G., Thomas, A., Grieser, J., et al.**, 2012. Global review and synthesis of trends in observed terrestrial near-surface wind speeds: implications for evaporation. *Journal of Hydrology* **416–417**, 182–205.
- Melton, F.A.**, 1940. A tentative classification of sand dunes its application to dune history in the southern High Plains. *Journal of Geology* **48**, 113–174.
- Miyaniishi, K., Johnson, E.A.**, 2021. Coastal dune succession and the reality of dune processes. In: Johnson, E.A., Miyaniishi, K. (eds.), *Plant Disturbance Ecology*. Elsevier, Amsterdam, pp. 253–290.
- Monaghan, G.W., Lovis, W.A., Fay, L.**, 1986. The Lake Nipissing transgression in the Saginaw Bay region, Michigan. *Canadian Journal of Earth Sciences* **23**, 1851–1854.
- Monmonier, M.**, 2002. Aerial photography at the Agricultural Adjustment Administration: acreage controls, conservation benefits, and overhead surveillance in the 1930s. *Photogrammetric Engineering & Remote Sensing* **68**, 1257–1261.
- Moore, L.J.**, 2000. Shoreline mapping techniques. *Journal of Coastal Research* **16**, 111–124.
- Morone, L.L.**, 1986. The observational error of automated wind reports from aircraft. *Bulletin of the American Meteorological Society* **67**, 177–185.
- Nield, J.M., Baas, A.C.W.**, 2008. The influence of different environmental and climatic conditions on vegetated aeolian dune landscape development and response. *Global and Planetary Change* **64**, 76–92.
- Nordstrom, K.F.**, 2015. Coastal dunes. In: Masselink, G., Gehrels, R. (Eds.), *Coastal Environments and Global Change*. John Wiley & Sons, Ltd., Hoboken, New Jersey, pp. 178–193.
- Olson, J.S.**, 1958a. Lake Michigan dune development 1. Wind-velocity profiles. *Journal of Geology* **66**, 254–263.
- Olson, J.S.**, 1958b. Lake Michigan dune development 2. Plants as agents and tools in geomorphology. *Journal of Geology* **66**, 345–351.
- Olson, J.S.**, 1958c. Lake Michigan dune development 3. Lake-level, beach, and dune Oscillations. *Journal of Geology* **66**, 473–483.
- Paskus, J.J., Enander, H.**, 2019. *Spatial Data to Improve Coastal Resiliency and Better Inform Local Decision-Making*. Michigan Natural Features Inventory, MNFI Report No. 2019-07, Lansing, MI.
- Peterson, J., Dersch, E.**, 1981. *Guide to Sand Dune and Coastal Ecosystem Functional Relationships*. Michigan State University Extension Bulletin EMICHU-SG-81-501, East Lansing, MI.
- Petty, W.P., Delcourt, P., Delcourt, H.**, 1996. Holocene lake-level fluctuations and beach-ridge development along the northern shore of Lake Michigan, USA. *Journal of Paleolimnology* **15**, 147–169.
- Phillips, J.D.**, 2006. Deterministic chaos and historical geomorphology: a review and look forward. *Geomorphology* **76**, 109–121.
- Phillips, J.D.**, 2007. The perfect landscape. *Geomorphology* **84**, 159–169.
- Pluis, J.L.A.**, 1992. Relationships between deflation and near surface wind velocity in a coastal dune blowout. *Earth Surface Processes and Landforms* **17**, 663–673.
- Provoost, S., Jones, M.L.M., Edmondson, S.E.**, 2011. Changes in landscape and vegetation of coastal dunes in northwest Europe: a review. *Journal of Coastal Conservation* **15**, 207–226.
- Pye, K.**, 1983. Coastal dunes. *Progress in Physical Geography: Earth and Environment* **7**, 531–557.
- Quinn, F.H.**, 2002. Secular changes in Great Lakes water level seasonal cycles. *Journal of Great Lakes Research* **28**, 451–465.
- Rango, A., Laliberte, A., Winters, C.**, 2008. Role of aerial photos in compiling a long-term remote sensing data set. *Journal of Applied Remote Sensing* **2**, 023541. <https://doi.org/10.1117/1.3009225>.

- Ranwell, D., 1958. Movement of vegetated sand dunes at Newborough Warren, Anglesey. *Journal of Ecology* **46**, 83–100.
- Rapinel, S., Clément, B., Magnanon, S., Sellin, V., Hubert-Moy, L., 2014. Identification and mapping of natural vegetation on a coastal site using a Worldview-2 satellite image. *Journal of Environmental Management* **144**, 236–246.
- Riksen, M.J.P.M., Goossens, D., 2007. The role of wind and splash erosion in inland drift-sand areas in the Netherlands. *Geomorphology* **88**, 179–192.
- Ritchie, W., 1972. The evolution of coastal sand dunes. *Scottish Geographical Magazine* **88**, 19–35.
- Robertson, C., Nelson, T.A., Boots, B., Wulder, M.A., 2007. STAMP: spatial-temporal analysis of moving polygons. *Journal of Geographical Systems* **9**, 207–227.
- Ruddiman, W.F., 2014. *Earth's Climate, Past and Future, Third Ed.* W.H. Freeman and Company, New York, 464 pp.
- Ruggiero, P., Hacker, S., Seabloom, E., Zarnetske, P., 2018. The role of vegetation in determining dune morphology, exposure to sea-level rise, and storm-induced coastal hazards: a U.S. Pacific Northwest perspective. In: Moore, L.J., Murray, A.B. (Eds.), *Barrier Dynamics and Response to Changing Climate*. Springer International Publishing, Cham, Switzerland, pp. 337–361.
- Sadahiro, Y., Umemura, M., 2001. A computational approach for the analysis of changes in polygon distributions. *Journal of Geographical Systems* **3**, 137–154.
- Sala, O.E., Parton, W.J., Joyce, L.A., Lauenroth, W.K., 1988. Primary production of the central grassland region of the United States. *Ecology* **69**, 40–45.
- Salisbury, E., 1952. *Downs & Dunes: Their Plant Life and Its Environment*. G. Bell & Sons, Ltd., London.
- Sanford, F.H., 1916. Michigan's shifting sands. Their control and better utilization. *Annual Report of the Agricultural Experiment Station, Michigan Agricultural College* **29**, 385–413.
- Schaetzl, R., Anderson, S., 2005. *Soils: Genesis and Geomorphology*. Cambridge University Press, New York.
- Schaney, M.L., Kite, J.S., Schaney, C.R., Thompson, J.A., 2021. Evidence of mid-Holocene (Northgrippian Age) dry climate recorded in organic soil profiles in the central Appalachian Mountains of the eastern United States. *Geosciences* **11**, 477. <https://doi.org/10.3390/geosciences11110477>.
- Schrotenboer, B.R., Arbogast, A.F., 2010. Locating alternative sand sources for Michigan's foundry industry: a geographical approach. *Applied Geography* **30**, 697–719.
- Schwarz, C., Brinkkemper, J., Ruessink, G., 2018. Feedbacks between biotic and abiotic processes governing the development of foredune blowouts: a review. *Journal of Marine Science and Engineering* **7**, 2. <https://doi.org/10.3390/jmse7010002>.
- Shay, J.M., Herring, M., Dyck, B.S., 2000. Dune colonization in the Bald Head Hills, southwestern Manitoba. *Canadian Field Naturalist* **114**, 612–627.
- Sherman, D.J., Bauer, B.O., 1993. Dynamics of beach-dune systems. *Progress in Physical Geography: Earth and Environment* **17**, 413–447.
- Short, A.D., 2012. Coastal processes and beaches. *Nature Education Knowledge* **3**, 15. <https://www.nature.com/scitable/knowledge/library/coastal-processes-and-beaches-26276621/>.
- Short, A.D., Hesp, P.A., 1982. Wave, beach and dune interactions in south-eastern Australia. *Marine Geology* **48**, 259–284.
- Sloss, C.R., Shepherd, M., Hesp, P.A., 2012. Coastal dunes: geomorphology. *Nature Education Knowledge* **3**, 2. <https://www.nature.com/scitable/knowledge/library/coastal-dunes-geomorphology-25822000/>.
- Smith, A.B., Jackson, D.W.T., Cooper, J.A.G., Hernández-Calvento, L., 2017. Quantifying the role of urbanization on airflow perturbations and dunefield evolution. *Earth's Future* **5**, 520–539.
- Smyth, T.A.G., Wilson, R., Rooney, P., Yates, K.L., 2022. Extent, accuracy and repeatability of bare sand and vegetation cover in dunes mapped from aerial imagery is highly variable. *Aeolian Research* **56**, 100799. <https://doi.org/10.1016/j.aeolia.2022.100799>.
- Theuerkauf, E., Mattheus, C.R., Braun, K., Bueno, J., 2021. Patterns and processes of beach and foredune geomorphic change along a Great Lakes shoreline: insights from a year-long drone mapping study along Lake Michigan. *Shore & Beach* **89**, 46–55.
- Thom, B., Hesp, P., Bryant, E., 1994. Last glacial "coastal" dunes in Eastern Australia and implications for landscape stability during the last glacial maximum. *Palaeogeography, Palaeoclimatology, Palaeoecology* **111**, 229–248.
- Thompson, T.A., Baedke, S.J., 1997. Strand-plain evidence for Late Holocene lake-level variations in Lake Michigan. *Geological Society of America Bulletin* **109**, 666–682.
- Thompson, T.A., Lepper, K., Endres, A.L., Johnston, J.W., Baedke, S.J., Argyllan, E.P., Booth, R.K., Wilcox, D.A., 2011. Mid Holocene lake level and shoreline behavior during the Nipissing phase of the upper Great Lakes at Alpena, Michigan, USA. *Journal of Great Lakes Research* **37**, 567–576.
- Thorn, C.E., Welford, M.R., 1994. The equilibrium concept in geomorphology. *Annals of the Association of American Geographers* **84**, 666–696.
- Tian, Q., Huang, G., Hu, K., Niyogi, D., 2019. Observed and global climate model based changes in wind power potential over the Northern Hemisphere during 1979–2016. *Energy* **167**, 1224–1235.
- Tojo, K., Udo, K., 2018. Analysis of beach recovery after the 2011 Tohoku Earthquake Tsunami based on shoreline extraction by ISODATA. In: Shim, J.-S., Chun, I., Lim, H.S. (Eds.), *Proceedings from the International Coastal Symposium (ICS) 2018 (Busan, Republic of Korea)*. *Journal of Coastal Research, Special Issue* **85**, 171–175.
- Torralba, V., Doblas-Reyes, F.J., Gonzalez-Reviriego, N., 2017. Uncertainty in recent near-surface wind speed trends: a global reanalysis intercomparison. *Environmental Research Letters* **12**, 114019. <https://doi.org/10.1088/1748-9326/aa8a58>.
- Tsoar, H., 2005. Sand dunes mobility and stability in relation to climate. *Physica A: Statistical Mechanics and its Applications* **357**, 50–56.
- Turner, M.G., Romme, W.H., Gardner, R.H., O'Neill, R. V., Kratz, T.K., 1993. A revised concept of landscape equilibrium: disturbance and stability on scaled landscapes. *Landscape Ecology* **8**, 213–227.
- Utrabo-Carazo, E., Azorin-Molina, C., Serrano, E., Aguilar, E., Brunet, M., Guijarro, J.A., 2022. Wind stilling ceased in the Iberian Peninsula since the 2000s. *Atmospheric Research* **272**, 106153. <https://doi.org/10.1016/j.atmosres.2022.106153>.
- Vachaud, G., Passerat De Silans, A., Balabanis, P., Vauclin, M., 1985. Temporal stability of spatially measured soil water probability density function. *Soil Science Society of America Journal* **49**, 822–828.
- van Dijk, D., 2004. Contemporary geomorphic processes and change on Lake Michigan coastal dunes: an example from Hoffmaster State Park, Michigan. *Michigan Academician* **35**, 425–453.
- van Dijk, D., 2014. Short- and long-term perspectives on the evolution of a Lake Michigan foredune. In: Fisher, T.G., Hansen, E.C. (Eds.), *Coastline and Dune Evolution Along the Great Lakes*. *Geological Society of America Special Paper* **508**, 195–216.
- Van Oort, M.D., Arbogast, A.F., Hansen, E.C., Hansen, B., 2001. Geomorphological history of massive parabolic dunes, Van Buren State Park, Van Buren County, Michigan. *Michigan Academician* **33**, 175–188.
- Vautard, R., Cattiaux, J., Yiou, P., Thépaut, J.-N., Ciais, P., 2010. Northern Hemisphere atmospheric stilling partly attributed to an increase in surface roughness. *Nature Geoscience* **3**, 756–761.
- Walker, I.J., Davidson-Arnott, R.G.D., Bauer, B.O., Hesp, P.A., Delgado-Fernandez, I., Ollerhead, J., Smyth, T.A.G., 2017. Scale-dependent perspectives on the geomorphology and evolution of beach-dune systems. *Earth-Science Reviews* **171**, 220–253.
- Wang, T., Zlotnik, V.A., Wedin, D., Wally, K.D., 2008. Spatial trends in saturated hydraulic conductivity of vegetated dunes in the Nebraska Sand Hills: effects of depth and topography. *Journal of Hydrology* **349**, 88–97.
- Warner, S., Jeffries, S., Lovis, W., Arbogast, A., Telewski, F., 2021. Tree ring-reconstructed late summer moisture conditions, 1546 to present, northern Lake Michigan, USA. *Climate Research* **83**, 43–56.
- Watras, C.J., Read, J.S., Holman, K.D., Liu, Z., Song, Y.-Y., Watras, A.J., Morgan, S., Stanley, E.H., 2014. Decadal oscillation of lakes and aquifers in the upper Great Lakes region of North America: hydroclimatic implications. *Geophysical Research Letters* **41**, 456–462.
- Werner, C.M., Mason, J.A., Hanson, P.R., 2011. Non-linear connections between dune activity and climate in the High Plains, Kansas and Oklahoma, USA. *Quaternary Research* **75**, 267–277.

- White, R.A., Piraino, K., Shortridge, A., Arbogast, A.F.**, 2019. Measurement of vegetation change in critical dune sites along the eastern shores of Lake Michigan from 1938 to 2014 with object-based image analysis. *Journal of Coastal Research* **35**, 842–851.
- Wilcoxon, F.**, 1945. Individual comparisons by ranking methods. *Biometrics Bulletin* **1**, 80–83.
- Wilson, S.E.**, 2001. *Michigan's Sand Dunes: An Michigan's Study of Coastal Sand Dune Mining in Michigan*. Geological Survey Division, Michigan Department of Environmental Quality, Lansing, Pamphlet 7. http://www.michigan.gov/documents/deq/PA07_304669_7.pdf.
- Wright, L.D., Thom, B.G.**, 1977. Coastal depositional landforms. *Progress in Physical Geography: Earth and Environment* **1**, 412–459.
- Yin, J., Han, W., Gao, Z., Chen, H.**, 2021. Assimilation of Doppler radar radial wind data in the GRAPES mesoscale model with observation error covariances tuning. *Quarterly Journal of the Royal Meteorological Society* **147**, 2087–2102.
- Yizhaq, H., Ashkenazy, Y., Tsoar, H.**, 2007. Why do active and stabilized dunes coexist under the same climatic conditions? *Physical Review Letters* **98**, 98–101.
- Yurk, B., Hansen, E.**, 2021. Effects of wind patterns and changing wind velocities on aeolian drift potential along the Lake Michigan shore. *Journal of Great Lakes Research* **47**, 1504–1517.
- Zeng, Z., Piao, S., Li, L.Z.X., Ciais, P., Li, Y., Cai, X., Yang, L., Liu, M., Wood, E.F.**, 2018. Global terrestrial stilling: does Earth's greening play a role? *Environmental Research Letters* **13**, 124013. <https://doi.org/10.1088/1748-9326/aaea84>.
- Zeng, Z., Ziegler, A.D., Searchinger, T., Yang, L., Chen, A., Ju, K., Piao, S., et al.**, 2019. A reversal in global terrestrial stilling and its implications for wind energy production. *Nature Climate Change* **9**, 979–985.
- Zhan, J., Maun, M.A.**, 1994. Potential for seed bank formation in seven Great Lakes sand dune species. *American Journal of Botany* **81**, 387–394.